16

Optical and Resonant Non-Linear Optical Properties of J-Aggregates of Pseudoisocyanine Derivatives in Thin Solid Films

Vladimir V. Shelkovnikov[1] and Alexander I. Plekhanov[2]
[1]*Novosibirsk Institute of Organic Chemistry SB RAS, Novosibirsk,*
[2]*Institute of Automation and Electrometry SB RAS, Novosibirsk,*
Russia

1. Introduction

The properties of colligative states of spontaneously aggregated polymethine dyes differ substantially from those of monomeric dye. Excellent examples of such self-organized molecular ensembles are J-aggregates of cyanine dyes. The J-aggregated state is now being considered for a number of non-cyanine dyes, the cyanine dye is still the most known and effective dye for J-aggregate formation (Wurthner, 2011). J-aggregates of cyanine dyes, first discovered by Jelley and Scheibe in 1936 (Jelley, 1936; Scheibe, 1936), have been studied for many years (Kobayashi, 1996). J-aggregates of cyanine dyes attract the attention of the researchers due to their interesting optical properties. J-aggregates are characterized by a strong absorption peak (J-peak) with narrow line widths which are bathochromically shifted relative to the absorption band of the monomeric dye. Their role as photographic sensitizers can hardly be overestimated (Tani, 1996; Trosken et al., 1995; Shapiro, 1994). Aggregates of dye molecules may be used to mimic light harvesting arrays and to prepare artificial photosynthetic systems (McDermott et al., 1995; Blankenship, 1995). Another development is the efficient electroluminescence revealed in single-layer light-emitting diodes based on electron-hole conducting polymers containing nano-crystalline phases of J-aggregates of cyanine dyes (Mal'tsev et al., 1999).

The promise in the property of J-aggregates lies in their high non-linear cubic optical susceptibility, $\chi^{(3)} \sim 10^{-7}$ esu, with a fast response time at the J-peak resonance in solutions and polymer films (Wang, 1991; Bogdanov et al., 1991).

The pseudoisocyanine dye (PIC) is the known dye which forms the J-aggregates in solutions. Of particular interest is the formation and non-linear optical properties of J-aggregates in thin solid films. Films of J-aggregates of organic dyes are promising nanomaterials for non-linear optical switches because they have the unique properties of high non-linear bleaching and non-linear refraction (Markov et al., 2000). As shown in Glaeske et al. (2001), films of J-aggregates with bistable behaviour may be the basis for two-dimensional optical switches, controllable by light. The non-linear optical properties of

organic dye J-aggregates have been intensively studied for application in future optical telecommunication and signal processing systems with ultrahigh bit rates (Tbit/s) (Furuki et al., 2000). The observed giant resonant third-order susceptibility in PIC thin solid films $\chi^{[3]}$~10^{-5}-10^{-4} esu (5 orders of magnitude greater than in polyconjugated polymers) and accessible production of optical quality films over a large area gives the possibility of J-aggregates application in telecommunication for terahertz demultiplexing of optical signals.

The methods for obtaining the J-aggregates in solutions do not give stable aggregates, which hampers their application as non-linear optical materials. Besides, a thin film geometry is preferable for applications. Therefore, the preparation of large area thin films of J-aggregates with thermal and photochemical stability, and high optical quality is vital for practical application and a matter of much current interest. The pseudoisocyanine at proper conditions efficiently forms J-aggregates in solid thin films (Shelkovnikov et al., 2002). The aim of this paper is to clarify the influence on the spectral linear and non-linear properties of PIC J-aggregates in thin solid films using a number of factors: structure of pseudoisocyanine dye derivatives, local field factor and character of J-peak broadening.

2. Experiments and discussions

2.1 Experimental part - Materials and methods

We used two methods to stimulate the J-aggregates' formation in the thin solid films. The use of a solution of PIC dyes with long alkyl substituents (Shelkovnikov et al., 2002) and the use of a PIC2-2 solution with the addition of cluster hydroborate anions (Shelkovnikov et al., 2004). Synthesis of the number of the derivatives of PIC with symmetrical and non-symmetrical long alkyl chain substituters for the physical-chemical experiments was carried out and the obtained dyes were isolated, chromatographically refined and characterized using the ^{1}H nuclear magnetic resonance method (Orlova et al., 2002; Orlova et al., 1995). Synthesis and characterization of the PIC2-2 derivative with cluster anion - closo-hexahydrodecaborate ($B_{10}H_{10}^{2-}$) by the infra-red spectroscopy and X-ray spectroscopy methods was carried out [Plekhanov et al., 1998a, 1998c; Cerasimova et al., 2000).

The thin solid films of PIC dye were prepared using spin-coating of the dye solution on the clean glass plates 2,5x2,5 cm^2 with a rate of rotation of 2000-3000 rpm on the custom made spin-coating equipment.

The linear optical spectra of the thin solid samples, depending on the experiments, were measured on the spectrophotometer Hewlett Packard 8453, fast fibre optics spectrophotometer Avantes AVS-SD2000 and fast fibre optics spectrophotometer Calibri VMK Optoelectronics, Novosibirsk (http://www.vmk.ru/). Fast spectrophotometers allow the measurement of 40 spectra per second. Sample heating for determination of the J-aggregates' thermal stability was done in a thermostatic optical chamber with a constant heating rate of 1.5 deg/min.

The thickness, dispersion of refractive index, and absorption of the obtained films were measured on a spectral ellipsometer Ellips developed at the A.V.Rzhanov Institute of Semiconductor Physics SB RAS (http://www.isp.nsc.ru/). The optical parameters of the film according to ellipsometric parameters delta (Δ) and psi (Ψ) were found by approximating the single-phase model of the Si-substrate/absorbing film.

The steady-state luminescence spectra were recorded on the Cary-Eclipse (Varian) and Hitachi 850 spectrofluorimeters. The kinetics of the luminescence decay was measured on the set-up of the Federal Institute for Materials Research and Testing (Berlin, Germany) with the assistance of researcher Ch. Spitz. The excitation was carried out in the cryostat by the pulse irradiation of the dye laser (R6G dye) with pulse duration 80ps synchronously pumped by pulse mode-locking Ar+ laser. The luminescence of the PIC J-aggregates was separated by monochromator and measured in the photon counting regime by the photo-multiplier.

The measurement of non-linear cubic susceptibilities of J-aggregates' PIC in thin solid films was carried out using the Z-scan method on the set-up shown on fig. 1 based on the dye R6G laser pumped using 5 ns pulsed Nd:YAG laser.

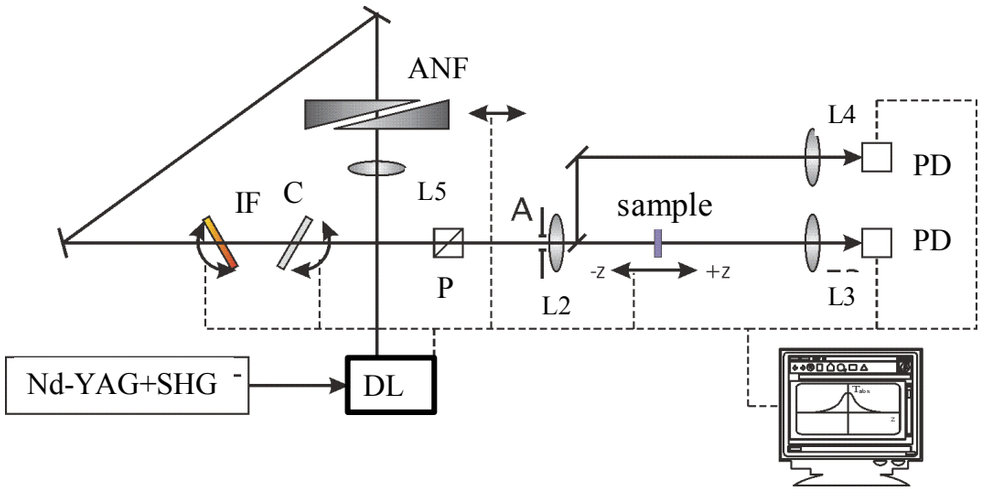

Fig. 1. Z-scan set-up. Nd-YAG+SHG – pulse laser, DL – Dye laser, L1-L4 –lenses, A – Aperture diaphragm, P – Glan prism, IF – interference filter, C– compensator of the beam shift, ANF– adjusted neutral filter, PD–photodiode.

The weak luminescence of the laser dye was cut off by the interference filter IF590 (Carl Zeiss Jena). The light signals were measured by photodiodes and the measured T(z) curves had 200 experimental points with the average value taken from the tens pulses. The calibration was carried out with etalon CS_2 substance (γ=(3.6±0.3)10^{-14} cm^2/W). The values of the real $Re^{(3)}$ and imaginary $Im^{(3)}$ parts of the cubic susceptibility in the esu units from the measured values' non-linear refraction coefficient γ and absorption coefficient β in SI units were calculated by equations:

$$\mathrm{Re}\,\chi^{(3)} = \frac{cn_0^2}{160\pi^2}\cdot\left(\gamma - \left(\frac{\lambda}{4\pi}\right)^2 \frac{\alpha_0\beta}{n_0}\right) \tag{1}$$

$$\mathrm{Im}\,\chi^{(3)} = \frac{\lambda cn_0^2}{640\pi^3}\cdot\left(\beta + \frac{\alpha_0\gamma}{n_0}\right) \tag{2}$$

where, c – light velocity in vacuum, λ - irradiation wavelength.

2.2 The formation of J-aggregates' PIC with the long alkyl chain substituters in thin solid films

The derivatives of PIC with symmetrical and non-symmetrical long alkyl chain substituters were synthesized to stimulate the J-aggregates' formation in thin solid films.

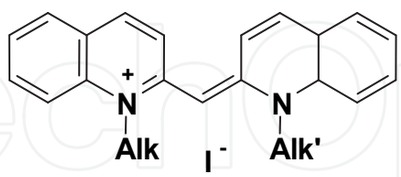

Alk=Alk'=C_2H_5 (PIC2-2), Alk=C_2H_5, Alk'=C_6H_{13}(PIC2-6),

Alk=Alk'=$C_{10}H_{21}$(PIC10-10), Alk=C_2H_5, Alk'=$C_{10}H_{21}$(PIC2-10),

Alk=Alk'=$C_{15}H_{31}$(PIC15-15), Alk=C_2H_5, Alk'=$C_{15}H_{31}$(PIC2-15),

Alk=Alk'=$C_{18}H_{37}$(PIC18-18), Alk=C_2H_5, Alk'=$C_{18}H_{37}$(PIC2-18).

There is no difference in the absorption spectra of the obtained dye in monomer form in organic solution. Symmetrical dyes do not give J-aggregated form in solid films and have the tendency to form H-aggregates. All non-symmetrical dyes with long alkyl chains PIC2-6, PIC2-10, PIC2-15, PIC2-18 give the J-aggregated form in thin solid films, see fig. 2, with maximum at λ=575-583 nm and FWHM 360-400 cm^{-1}.

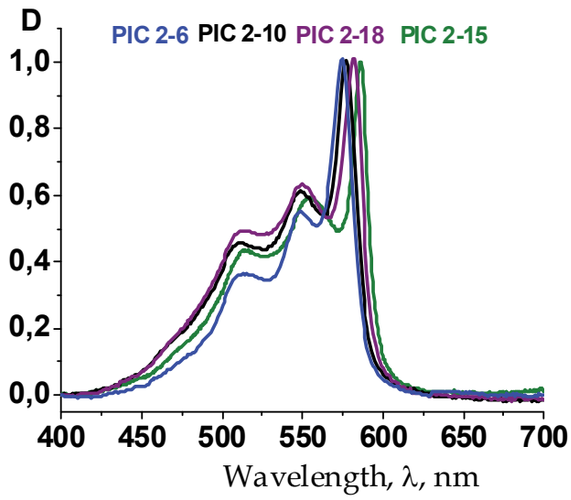

Fig. 2. The absorption spectra of the non-symmetrical pseudoisocyanines in thin solid films.

There are three electron-phonon transitions (526, 492 и 460 nm) shifted relative to each-other to the quant of the double C=C bound oscillation (1400 cm^{-1}) for the monomer form of dye in the solution. The same three transitions shifted to the long wave side are observed in the structural absorption band with the maximum at 556 nm in the spectra of the non-symmetrical pseudoisocyanines in the thin solid films. This band did not change at the

thermal decay of the J-aggregate and belongs to the monomer form of the dye. Thus, the spectrum of dye in solid films is the superposition of monomer and J-aggregated forms.

The absorption in the maximum of the J-aggregates' peak exceeds the absorption in the maximum of the monomer form by as much as 1.5-1.8 times. The relation of the optical density in the J-aggregates' peak and in the monomer maximum (J/M) was used to characterize the degree of the conversion dye to aggregate in thin solid films. The length of the alkyl chain has a weak dependence on the degree of the conversion of the monomer to the J-aggregate in the thin solid films. But the alkyl chain length has a strong influence on the rate and degree of the spontaneous recovering of the J-aggregate after thermal destruction. For example, the J-aggregate of PIC2-2 did not restore at all. The recovering begins after 4 day storing in the box at humidity 80% for the J-aggregate of PIC2-6. The J-aggregate of PIC2-10 restored to 80% after a day of storing and PIC2-15 after 12 hours of storing. The J-aggregate of PIC2-18 is completely restored during 4 hours at room temperature. The increase of the alkyl chain length leads to an increasing degree of restoration and shortening of the time of restoring by order of magnitude. To stabilize the J-aggregates on the substrate, a dye with long alkyl substituters is useful. Such substituters lead to an efficient J-aggregation at room temperature, but the aggregates are unstable upon an increase in temperature above 60°C.

2.3 The spectrophotometry of the thermal decay of PIC J-aggregates with long alkyl substituters

The J-aggregates of the PIC with long alkyl substituters are thermally destroyed with transition to the monomer form. The thermal conversion of the J-aggregates of pseudoisocyanine derivatives is studied by measurement of optical absorption spectra at continuous increase of temperature. The spectral change of the J-aggregates of PIC2-18 in the thin film with temperature increased is shown in fig. 3.

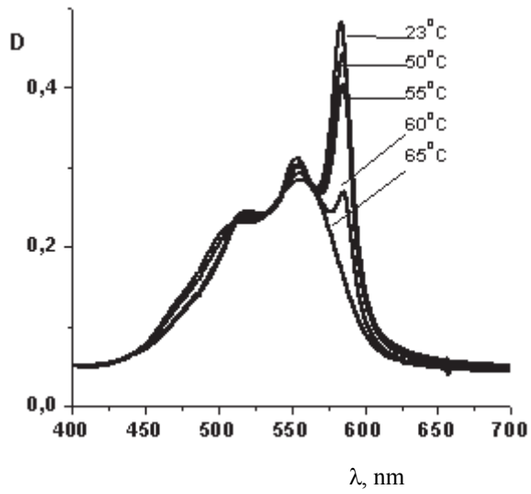

Fig. 3. The spectral change of the J-aggregated film PIC2-18 at sample heating

The J-peak disappears at temperatures above 60^0C and the finished spectrum looks like the broadening spectrum of the monomer form of the dye. The J-aggregates' thermal decay

curves are plotted (see fig. 4) and from this it is shown that dyes line to the next row of thermal stability determined on the point of inflection of the thermal decay curve: PIC2-2 (73°C) > PIC2-6 (67°C) > PIC2-18 (55°C) > PIC2-10 (47°C) > PIC2-15 (37°C).

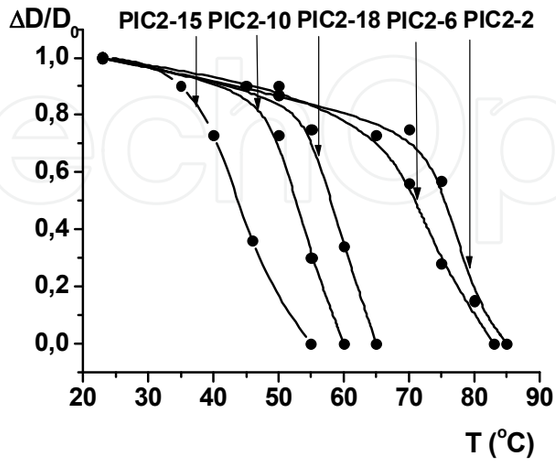

Fig. 4. The thermal decay curves of the J-aggregates of the non-symmetrical dyes in the thin solid films

The effective energies of activation of thermal decay of J-aggregates in thin films were calculated from the non-isothermic curves of the thermal decay. The degree of J-aggregate thermal decay (α_J) is $\frac{d\alpha_J}{dt} = k \cdot \left(1 - \alpha_J\right)$

Where, $k = Z \cdot \exp\left(-\frac{E_a}{RT}\right)$; Z - preexponential factor, E_a – activation energy, T – temperature.

The differential equation for the degree of thermal decay at constant rate of heating is (Wendlandt, 1974)

$$\frac{d\alpha_J}{dT} = \frac{Z}{\beta} \cdot \left(1 - \alpha_J\right) \cdot \exp\left(-\frac{E_a}{RT}\right) \tag{3}$$

Where, β – the rate of the sample heating (dT/dt). After integration we have

$$\alpha_J = 1 - \exp\left(-\left(\frac{Z}{\beta} \cdot \frac{RT^2}{E_a} \cdot \left(1 - \frac{2RT}{E_a}\right) \cdot \exp\left(-\frac{E_a}{RT}\right)\right)\right) \tag{4}$$

The dependence of the $\left(\ln\left[-\ln\left(1-\alpha_J\right)\right]\right)$ vs. $1/T$ gives the value E_a from this equation. The experimental and theoretical curves of $\alpha_J(T)$ and double-logarithmic line are shown in fig. 5 for the case of PIC-2-15 J-aggregates' thermal decay.

The obtained values of activation energy for the thermal decay of the J-aggregates of PIC with different long alkyl chains are shown in table 1.

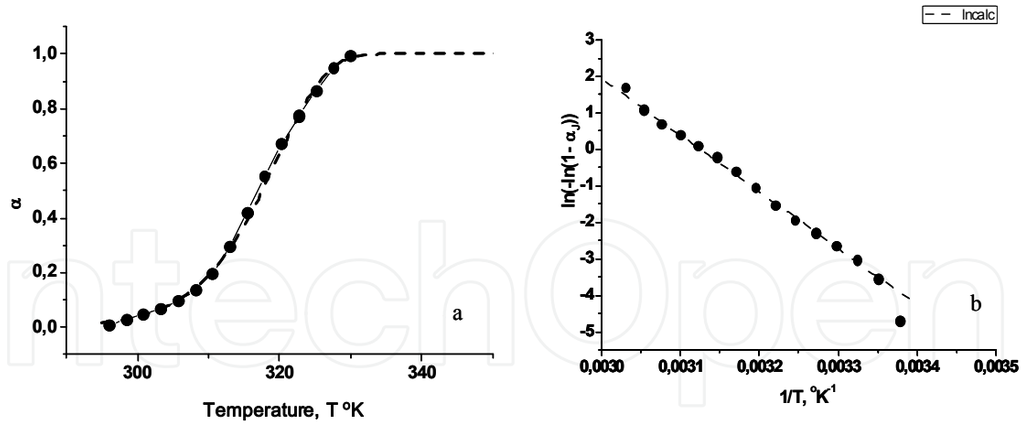

Fig. 5. a,b. Experimental (points) and the model (dash) curves of the degree of the J-aggregates' PIC2-15 thermal decay (a) and its linear approximation vs 1/T

Dye	E_a *kcal/mol*
PIC 2-2	43
PIC 2-6	30
PIC 2-10	39
PIC 2-15	30
PIC 2-18	41

Table 1. The values of the activation energy for the thermal decay of the J-aggregates in the thin solid films

We can conclude that the average value of the effective activation energy for the thermal decay of the J-aggregates in the thin solid film is 36 kcal/mol. Let us compare the value of the effective activation energy for the thermal decay of the J-aggregates with the electrostatic energy of the PIC dimer formation. The main contribution to the dimerization energy gives the Coulomb interaction of the two PIC cations and halogen anions (Krasnov, 1984).

$$E_{ion} = -\frac{q_1 \cdot q_2}{r} + A \cdot \exp\left(-\frac{r}{\rho}\right) \tag{5}$$

Where, q_1 and q_2 are charges of ions, r – the distance between ions, A – the coefficient that characterizes the energy of repulsive exchange interactions of the electron orbitals and ρ is the constant equal 0,34 Å. The A value is calculated from the minimum ($\frac{\partial E}{\partial r} = 0$) of the cation-anion interaction.

$$A = -\frac{q_1 \cdot q_2 \cdot \rho}{r^2_{\min}} \cdot \exp\left(\frac{r_{\min}}{\rho}\right) \tag{6}$$

The value of the energy of the dimer is the minimal at quadruple replacement of the cations and anions as shown in fig. 6. In this case the electrostatic energy of the dimer is

$$E_D = -\frac{4 \cdot q_{PIC} \cdot q_{an}}{r} + 4 \cdot A \cdot \exp\left(-\frac{r}{\rho}\right) + \frac{q^2{}_{PIC}}{r \cdot \sqrt{2}} + \frac{q^2{}_{an}}{r \cdot \sqrt{2}} + 2 \cdot A \cdot \exp\left(-\frac{r \cdot \sqrt{2}}{\rho}\right) \quad (7)$$

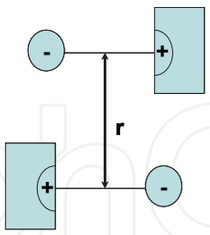

Fig. 6. Quadruple model of the PIC dimer

The effective positive charge of the dye (q_{PIC}~+0,7) and the value of the equilibrium distance cation-anion in the PIC molecule (3 Å) were determined from the quantum chemical calculation using the AM1 method. The map of the calculated electrostatic potential of the PIC iodide is shown in fig. 7.

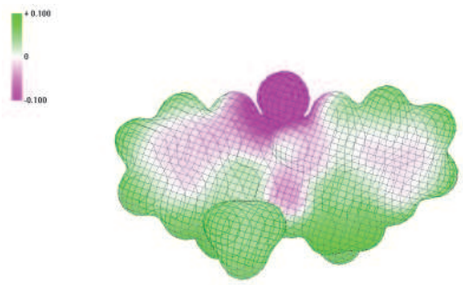

Fig. 7. Electrostatic potential map of the PIC iodide molecule

The value of the dimerization energy was calculated as the difference between the dimer energy and the two molecules PIC in the monomer form.

$$E_D = -\frac{2 \cdot q_{PIC} \cdot q_{an}}{r} + 2 \cdot A \cdot \exp\left(-\frac{r}{\rho}\right) + \frac{q^2{}_{PIC}}{r \cdot \sqrt{2}} + \frac{q^2{}_{an}}{r \cdot \sqrt{2}} + 2 \cdot A \cdot \exp\left(-\frac{r \cdot \sqrt{2}}{\rho}\right) \quad (8)$$

The molecules' distance depending on the dimerization energy is shown in fig. 8.

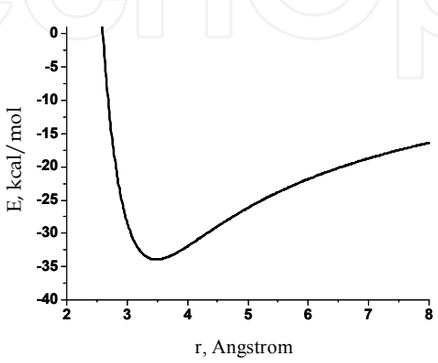

Fig. 8. Distance dependence of the PIC halogen dimerization energy

The minimum of the curve is -34 kcal/mol with the equilibrium distance between PIC molecules 3,5 Å. This is in good agreement with Van der Waals' distance in the dyes' dimers. One can see that the energy of the calculated value of energy of the pair electrostatic interaction of PIC (-34 kcal/mol) is close to the average value of the effective activation energy for the thermal decay of the J-aggregates' PIC (-36 kcal/mol).

The value of the enthalpy of the dyes dimerization in the solution is 6-12 kcal/mol (Ghasemi & Mandoumi, 2008; Coates, 1969; Nygren et al., 1996). It is less than the calculated energy of the dimerization PIC due to the compensatory contribution of the high energy of the dye solvatation. That means that in the solution or in the solvatating polymer the thermal decay of the J-aggregates will happens much more easily than in a non-solvating polymer or in solid films.

2.4 The spectrophotometry of the J-aggregate PIC2-18 iodide to monomer conversion in thin film with the addition of 1-octadecyl-2-methylquinolinium

The number of monomer units in the J-aggregate PIC is an important characteristic in understanding its optical and non-linear optical properties in thin solid films. There are different opinions in the literature about the number of molecular units making up the aggregate: from hundreds (Sundstrom et al., 1988; Tani et al., 1996), tens (Daltrozzo et al., 1974), four (Herz, 1974) or three (Struganova, 2000) molecules in the J-aggregate PIC. Here we describe the difference between the number of molecules which can be in the J-aggregate as in a physical object, for an example in the micelle, and the minimal number of molecules which is enough to give the J-peak in the optical spectrum.

We use another organic cation 1-octadecyl-2-methylquinolinium (MQ18), which has the same charge (+1) and long alkyl tail as PIC2-18, to divide the PIC2-18 molecules in the J-aggregate in a thin solid film. In this way it is possible to determine the number of PIC2-18 molecules in the J-aggregate.

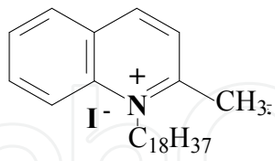

MQ18

The MQ18 is similar to one half of PIC2-18 and statistically replaces the PIC2-18 molecules at the moment of fast J-aggregate assembling during the short time of film formation during spin-coating. In this case the numbers of PIC2-18 molecules in the J-aggregate will depend on the relationship between the concentration of the MQ18 and dye in the film. The probability of PIC2-18 molecule substitution by MQ18 molecule (F_{MQ18}) in the film is equal to the part of the MQ18 molecules in the joint composition PIC18 and MQ18

$$F_{MQ18} = [C_{MQ18}]/([C_{MQ18}]+[C_{PIC18}]) \quad (9)$$

The absorption spectra of the films prepared by spin-coating on the basis of mixture PIC2-18:MQ18 (1:0.05,1:0.1, 1:0.2, 1:0.3, 1:0.5, 1:1) were measured and part of them is shown in fig. 9.

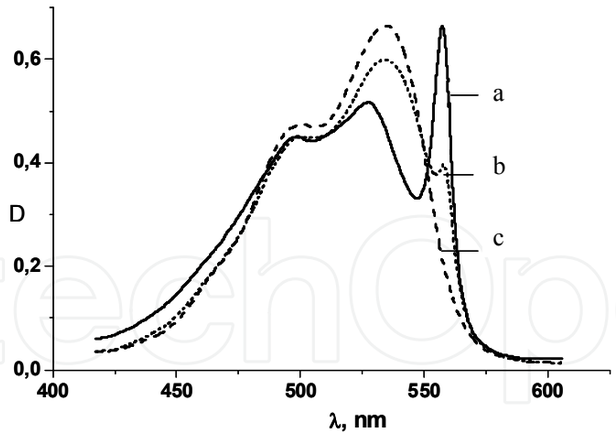

Fig. 9. The film spectra PIC2-18 at MQ18 addition in the mole relation 1:0 (*a*), 1:0.5 (*b*), 1:1(*c*)

One can see the transformation of the J-aggregate spectrum to the monomer dye spectrum with increasing the MQ18 concentration. At the molar relation PIC2-18:MQ18 1:1 we observe only the monomer form of dye. The part of the destroyed J-aggregates (F_J), which is determined as the change of the J-peak optical density ($(D^J_0 - D^J_{MQ18})/D^J_0$) is equal to the probability of the PIC2-18 molecule substitution multiplied by the number molecules (N) needed for J-peak appearance.

$$F_J=(D^J_0 - D^J_{MQ18})/\ D^J_0=N^* F_{MQ18} \tag{10}$$

The value N was calculated from the tangent of the (F_J-F_{MQ18}) dependence shown in fig. 10 is 2.6±0.2. This is between two and three. In accordance with the exciton description of supramolecular assemble (Malyshev, 1993) at the number of molecules in the J-aggregate, at more than two there should be noticeable a hypsochromic shift of J-peak as the aggregate decreases. The J-peak energy depending on the number of molecules in the J-aggregate is:

$$E_k = h\nu + 2V\cos\left(\pi k/\left(N+1\right)\right) \tag{11}$$

where $h\nu$ is the energy of the optical transition of the monomer dye, V – the dipole-dipole interaction of the neighbour molecules in the aggregate, N – the number of molecules in the J-aggregate. The spectral shift for the Lorenz contour of the J-peak (Lr_{ex}) was calculated for the number of PIC molecules in the J-aggregate from 2 to 5 (fig. 11).

$$Lr_{ex} = \frac{\Delta\nu \cdot 1/\sqrt{N}}{4\cdot\left(\frac{10^7}{\lambda} - \left(\nu_0 - \cos\left(\frac{\pi}{N+1}\right)\cdot 2V\right)\right)^2 + \left(\Delta\nu \cdot 1/\sqrt{N}\right)^2}\cdot N \tag{12}$$

Where, $\Delta\nu$ -the width of J-peak (300 cm^{-1}), ν_0 -maximum of the J-peak absorption (18770 cm^{-1}), V – 660 cm^{-1}.

The decreasing number of molecules from three to two in the J-aggregate leads to the blue shift of the spectra to 9 nm. In our case the J-peak disappeared, but the blue spectral shift

was not observed. It could be explained in the case of the J-aggregate dimer form presence. The dimer form of the dye was determined as the main form for the PIC J-aggregate.

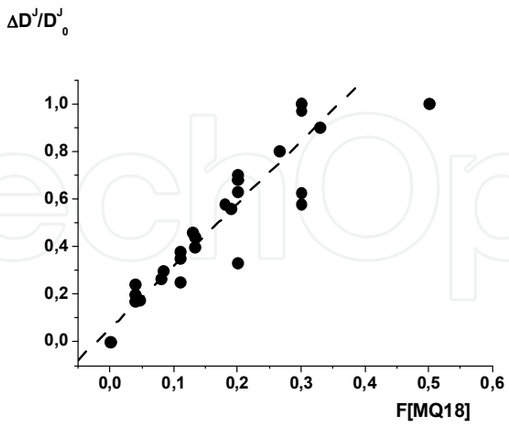

Fig. 10. The relative J-peak optical density change depending on the relative MQ18 content

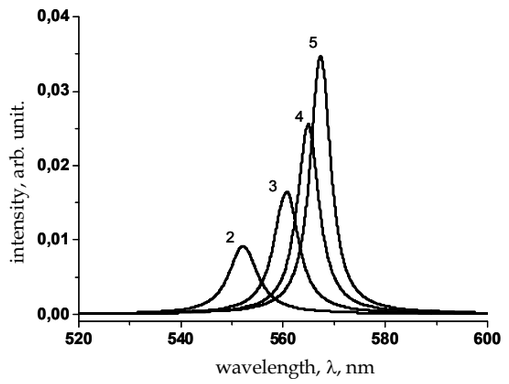

Fig. 11. The absorption spectra of the J-aggregate calculated using eq. 12 for the different number of the molecules in the J-aggregate (the curve number)

2.5 The optical constants of thin solid films of PIC derivatives

The frequency dispersion of the absorption coefficient k and the refractive index n of the films of PIC long chain derivatives in J-aggregated and monomer forms were determined in the wavelength region from 500 to 650 nm. The typical value of measured thin films thickness was 20-30nm. As an illustration, the resulting spectra for two films are shown in Fig. 12. The spectra for other films were similar. One shows anomalous dispersion for n within the region of dye absorption (500-570 nm), with the values n = 3.05 and k = 0.8 at the maximum of the J-peak dispersion curve; at the absorption maximum of the J-peak, n = 2.5 and k = 1.25 for film 21 nm thick.

The value of the index of absorption ($\alpha = 4\pi k / \lambda$) in thin solid films for PIC2-18 is: in the maximum of anomalous dispersion refraction $\alpha = 2,5 \cdot 10^5$ cm^{-1} for J-aggregate, $\alpha = 1,15 \cdot 10^5$ cm^{-1} in the maximum of absorption for monomer dye (n_{max}=2.1). The electron polarizability for J-aggregated (ρ_J) and monomer forms (ρ_m) of dye were calculated by extrapolation of the

refractive index of dispersion curve to infinite wavelength $n\infty$ using the least squares method and the Zelmeer equation (Verezchagin, 1980).

$$n_\infty = \sqrt{n - \frac{C}{\left(\lambda^2 - \lambda_0^2\right)}} \tag{13}$$

Where, C is constant, λ_0 – wavelength of J-peak maximum.

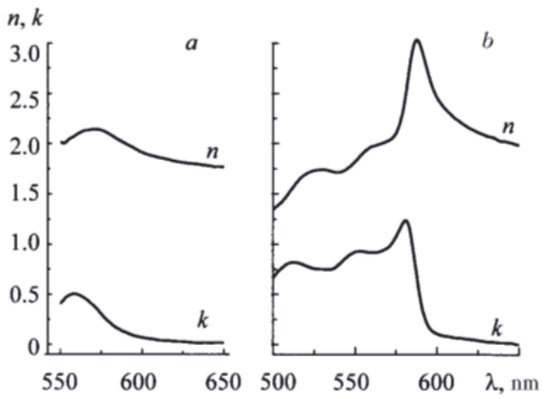

Fig. 12. Refractive indices (*n*) and absorption (*k*) of film of PIC 2-18 in the monomeric (a) and J-aggregated (b) form as functions of dispersion measured by spectral ellipsometry

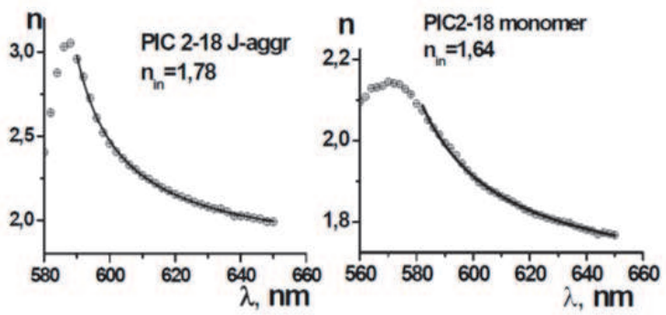

Fig. 13. Dispersion curves for PIC J-aggregate (a) and monomer (b) in the solid film (points) and their least square Zelmeer approximation (line)

The results of the dispersion curves' approximation of J-aggregated and monomer forms of PIC are shown on in fig 13. One can see a good consequence of experimental and fitted curves outside of resonance. The value refractive index for the PIC monomer in film is $n_{\infty m}$=1,64 and for J-aggregate is $n_{\infty J}$=1,78. The values of the electron polarizability (ρ) is obtained by equation

$$\rho = \frac{3}{4\pi N_A} \frac{n_\infty - 1}{n_\infty^2 + 2} \cdot \frac{M}{d} \tag{14}$$

Where ***M*** is molecular weight (consider dimer value for J-aggregate), ***d*** is density of molecules;

gives the values ρ_J=88 Å^3 for the J-aggregate and ρ_m=66 Å^3 for the monomer form of dye. The electron polarizability of the J-aggregate is 1.33 times more than the polarizability of the monomer. This is not too much to consider the electron delocalization in J-aggregate over the number of dye molecules, but rather it confirms some expansion of electron delocalization due to dye dimerization.

2.6 The luminescent properties of J-aggregate PIC with long alkyl chain

Resonance luminescence takes place for the J-aggregates' PIC in solutions. For example, the PIC forms the J-aggregates in water solution in the presence of phospholipide vesicles with the J-peak of absorption at 580 nm and the J-peak of the luminescence at 582 nm (Sato et al., 1989). The resonance luminescence corresponds to the absence of the molecular coordinate shift between the ground and the excited states' electron energy curves for the $\mathbf{S}_{00}$ and $\mathbf{S}^*_{00}$ oscillatory states. For the number of samples in solutions, the long wavelength luminescent wing with a maximum of 600-630 nm was observed for J-aggregates at a low temperature (Vacha et al., 1998; Katrich et al., 2000). The authors connect the reason for the long wavelength luminescence with the availability of the dimeric nature traps which accept the excitation energy of the J-aggregate.

The measured steady-state spectra of the luminescence of solid films of J-aggregated dyes PIC2-6, PIC2-10, PIC2-15 at room temperature are shown in fig. 14. The determined Stokes shift for the ν_{00}=1/2($\nu^{abs}_{\max} - \nu^{fl}_{\max}$) transition frequency is 90-100 см$^{-1}$ (see table 2). The measured spectra of the monomer PIC luminescence in water:ethanol (1:1) at concentration 10^{-4} *M/l* is shown in fig. 15. The spectrum has the band with broadening counter reaching 700 nm with the maximum at 565 nm. The Stokes shift for the monomer luminescence is 780 cm^{-1}. In accordance with the Lippert approach, the luminescence Stokes shift of the molecule in the medium appears due to the reaction of the medium which is described by the medium function ($f(\varepsilon,n)$) on the dipole moment change at the molecule excitation. The luminescence Stokes shift depends on the polarization function of medium and the square of change of the dipole moment in ground (M_g) and excited state (M_e) divided by the radius of the solvated molecule (R_a) in cube (Levshin & Salecky, 1989; Lakowics, 1983).

$$\Delta E_{st} = 2\frac{(M_e - M_g)^2}{R_a{}^3}\cdot\left[\frac{(\varepsilon-1)}{(\varepsilon+2)} - \frac{(n^2-1)}{(n^2+2)}\right]\cdot\frac{(2n^2+1)^2}{(n^2+2)^2} \tag{15}$$

The value of the radius of molecule solvate interaction was calculated from

$$R_a = \sqrt[3]{\frac{M}{d}\cdot\frac{3}{4\pi N_A}} \tag{16}$$

Where, M, d is the corresponding molecular weight and density of the dye. The obtained value R_a for PIC is R_a=4.5 Å. The calculation of R_a from the molecular volume of PIC cation (14.52x6.41x4.3=400 Å^3) gives the same value 4.57 Å. The value the radius of molecular cavity for PIC dimer is R_a = 5.66 Å.

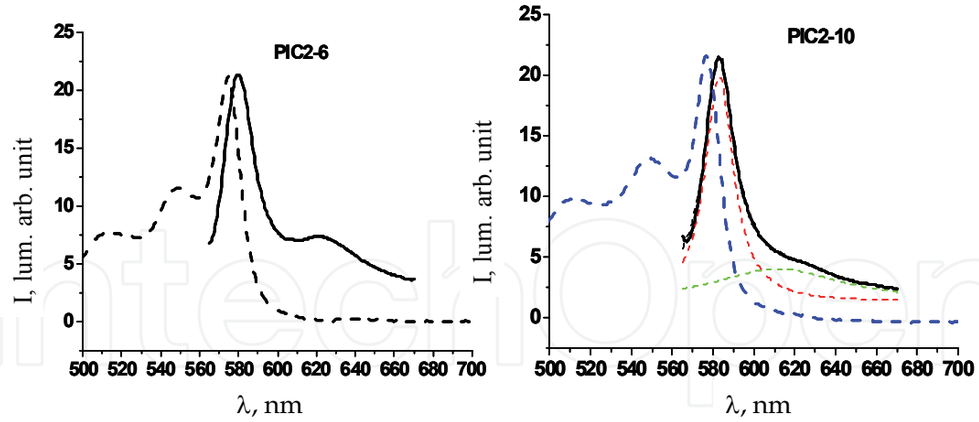

Fig. 14. a,b. The excitation and luminescence spectra in the thin solid films PIC2-6 (a), PIC2-10 (b) with two counter resolution

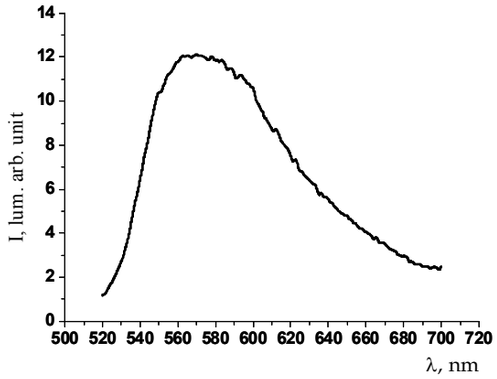

Fig. 15. The luminescence spectrum of the monomer PIC in the water-ethanol solution

Dye,ex. 550 nm	$\lambda_{Макс}$ I lum.,nm	$\nu_{max.abs}$- $\nu_{max.lum}$	Stokes shift, $\Delta\nu_{0\text{-}0}$, cm^{-1}	Lorenz counter lum. broadening , cm^{-1}	$\lambda_{Макс.}$ 2 lum., nm
PIC2-6	580	150	90	546	624
PIC2-10	583	140	93	502	611
PIC2-15	592	130	102	524	615

Table 2. The luminescent characteristics of the J-aggregates with long alkyl substituters in the thin solid films

The calculation of the dipole moment change for the PIC molecule from the obtained value of the Stokes shift in water-ethanol solution gives the value $\Delta\mu$=2.56D. The analogous calculation for the PIC dimer was carried out in water at Stokes shift 30 cm^{-1} is taken from (Sato et al., 1989) and gives the value $\Delta\mu$=0.7D. One can see from the values of $\Delta\mu$ that the difference of the dipole moments at ground and excited state decreases in 3.66 times with the conversion monomer to J-aggregate form of dye. The calculation of the $\Delta\mu$ change at

aggregation PIC at low temperature from the values of the Stokes shift (Renge & Wild 1997) gives the decreasing $\Delta\mu$ at aggregation by 5.5 times. In accordance with the symmetry of the PIC molecule, the dipole moments of the ground and excited state are directed along the short axe of the molecule. It is reasonable to propose that the decreasing of the dipoles moments at the aggregation (dimerization) takes place in the ground and excited state of the aggregate. The decreasing of the dipole moment by 3.7 times is possible at the contra-directed arrangement of the PIC molecules dipoles with the angle between dipoles 43°.

The decreasing of the $\Delta\mu$ apart from the decreasing of the Stokes shift of the luminescence leads to the decreasing of the inhomogeneous broadening of the J-aggregate peak in comparison with the broadening of the dye monomer form absorption band. The square of the inhomogeneous broadening of the molecular spectrum in the medium σ^2_{in} connected with the dipole moment change is proportional to the $\Delta\mu^2/R_a^3$ (Bakhshiev et al., 1989). The decreasing of the $\Delta\mu$ and increasing of the R_a at the dimerization of the dye leads to the decreasing of the inhomogeneous broadening in J-aggregate and the narrowing of the J-peak by 5-7 times in comparison with the spectral width of the monomer form of the molecule. The spectral shift between the maximum of the absorption and luminescence spectra ($\Delta\nu_{a,f}$) depends on the mean-square dispersion of the inhomogeneous broadening of the luminescence spectra of the molecules in the medium σ^2_{in} that corresponds to half width of the inhomogeneous broadening of the luminescence spectrum.

$$\sigma^2_{\phi\lambda} = \frac{kT}{hc} \cdot \Delta\nu_{a,f} \tag{17}$$

The experimental value ($\nu^{abs}_{\max} - \nu^{fl}_{\max}$) for J-aggregate PIC2-10 is 140 cm^{-1} (see table 2). The calculation of σ^2_{in} for luminescence spectrum of J-aggregates with long alkyl substituters in thin solid films gives a value of full width of inhomogeneous broadening luminescence contour $2\sigma_{in}$=338 cm^{-1}. The comparison of the obtained value $2\sigma_{in}$ (338 cm^{-1}) and experimental value FWHM for luminescence Gauss contour of J-aggregates in thin film 2σ=417 cm^{-1} allows us to conclude that the luminescence spectrum of the J-aggregates has essential contribution of orthe inhomogeneous broadening makes the essential contribution to the luminescence spectrum of the J- aggregates.

The wide long wavelength shoulder of the luminescence is observed on the all measured samples of the J-aggregated dyes in thin films, apart from the main luminescence peak. The maximum of that luminescence is at 610-625 nm depending on the sample and luminescence slump last to 670 nm. The expansion of the PIC2-10 luminescence spectrum on the two Lorentz contours is shown in fig. 14. On the basis of the measured excitation spectra, it was shown that the long wavelength luminescence does not have its own excitation band and its excitation spectra coincide with the absorption and excitation spectra of the J-aggregate. The long wavelength unstructured wide band in J-aggregated films luminescence we attribute to the exciplex luminescence between J-aggregate and monomer dye or between J-aggregates.

The life time of the exciplex luminescence as a rule is longer than the life time of the luminophore luminescence and has the period of luminescence signal growth relates to the stage of the closing in the molecular contact to form the exciplex. The measurement of the kinetics of the luminescence in the maximum of the long wavelength luminescence 625 nm

at room temperature shows the signal growing (see fig. 16) with characteristic time 2.1 ns and luminescence decay with life time 3.6 ns. The luminescence life time in the maximum of the J-aggregate has two components: the short component with life time 20-40 ps and the long component with life time 2.0 ns. One can see that the J-aggregate exciplex luminescence has the period of the signal growing and its life time is more than life time measured in the main peak of the J-aggregate luminescence.

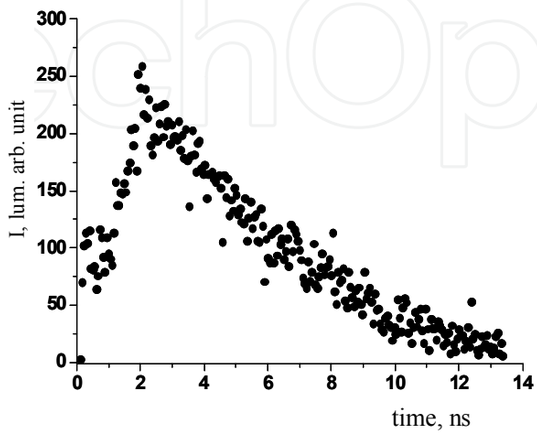

Fig. 16. Kinetics of the luminescence decay of the PIC2-15 at 625 nm in the thin film at the excitation on λ=*574* nm

2.7 The formation of J-aggregate PIC in thin solid films. The influence of the cluster anionic derivatives of high boron hydrides

One can see from the map of the electrostatic potential of PIC (fig. 7) that the positive charge of the molecule is distributed in the cavity of electrostatic potential where the anion is situated. From this for the stabilization of the PIC dimer the proper choice is a dianion with dipolar distribution of the negative charge. Cluster dianions of high boron hydrides have the dipolar distribution of the negative charge. The formation of the PIC J-aggregates with the addition of the some cluster high boron hydrides ($K_2B_{10}H_{10}$, $K_2B_{12}H_{12}$, $Cs_2B_{20}H_{18}$, $[Ni^{IV}(1,2\text{-}B_9C_2H_{11})_2]^0$, $Cs[Ni(1,2\text{-}B_9C_2H_{11})_2]$, $NH(CH_3)_3B_9C_2H_{12}$, $NH(C_2H_5)_3[Co(1,2\text{-}B_9C_2H_{11})_2]$, $Cs_2B_{10}H_8I_2$, $[Sn(1,2\text{-}B_9C_2H_{11})]^0$) was studied (Shelkovnikov et al., 2004). It was shown that the addition of anions of high boron hydrides $B_{10}H_{10}^{2-}$ and $B_{10}H_8I_2^{2-}$ to the PIC2-2 spin-coating solution at molar ratio dye:anion salt 1:0.1 leads to the effective formation of J-aggregates of dye in solid films. The absorption spectra of PIC films doped with $[Ni^{(IV)}(1,2\text{-}B_9C_2H_{11})_2]^0$, $[Sn(1,2\text{-}B_9C_2H_{11})]^0$ and anions $B_{10}H_{10}^{2-}$ *и* $B_{20}H_{18}^{2-}$ are shown in fig. 17. The J-peak is distinctly seen in the absorption spectra of the PIC films doped with $B_{10}H_{10}^{2-}$ anions. This anion leads to an efficient J-aggregation of PIC with the formation of stable J-aggregates in solid films.

Similarly to the $B_{10}H_{10}^{2-}$ anions, the addition of the neutral complex of nickel stimulates the predominant formation of J-aggregates of PIC in a solid film (*J*/*M*=1.52). The addition of the $B_{10}H_8I_2^{2-}$anion at holding times prior to centrifugation of more than 10 min leads to the formation of stable J-aggregates (*J*/*M* = 1.46). At short holding times prior to centrifugation (less than 5 min), a long wavelength shoulder located at 625 nm and extending up to 800 nm

was observed in the absorption spectra (Fig. 18). In this case, the optical density of the J-peak decreases. When a film doped with $B_{10}H_8I_2^{2-}$ anions is applied to a glass surface treated with a silicon-containing surfactant for the surface wettability improvement, a high conversion of the monomer to J-aggregates (J/M = 2.2) is observed (Fig. 18, spectrum *3*).

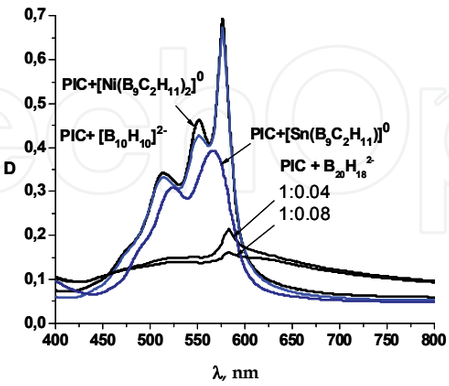

Fig. 17. Absorption spectra of PIC films doped with (1) $[Ni^{IV}(1,2\text{-}B_9C_2H_{11})_2]_0$, (2) $[Sn(1,2\text{-}B_9C_2H_{11})]^0$, (3) $B_{10}H_{10}^{2-}$ and (4, 5) $B_{20}H_{18}^{2-}$. Dye–anion mole ratio: (4) 1 : 0.04; (5) 1 : 0.08

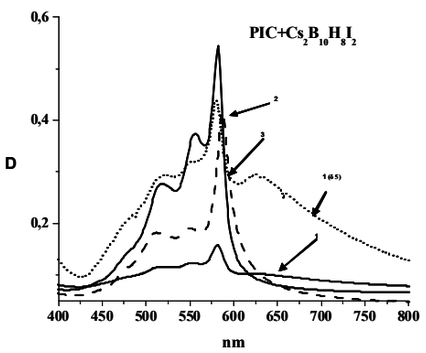

Fig. 18. Absorption spectra of PIC films doped by $B_{10}H_8I_2^{2-}$ anions. The holding time prior to centrifugation: (*1*) 2–3 min; (*2*, *3*) longer than 10 min. Sample *2* on a pure glass substrate; sample *3*, a glass substrate treated with a surfactant

A high stability of the J-aggregates of PIC-closo-hydrodecaborate allowed us to perform an additional doping of the dye film with organic cation salts without destroying the J-peak. The following salts of organic cations were used: methylcholine iodide, tetrabutylammonium (TBA) iodide, laurylcholine iodide and dodecylpyridine iodide. The salts of organic cations were introduced into the films at a mole ratio of the dye cation:added cation varying from 1 : 0.5 to 1 : 5. Upon an increase in the concentration of an organic cation to the mole ratio dye–cation 1 : 4, the J-peak increases in intensity and narrows by 1.5–2 times, as is shown in Fig. 19 for the case of TBA. At a higher concentration of organic cations in the film, the J-peak decays. The destruction of the J-aggregates was observed only upon a high dilution of a dye film with organic cations. This demonstrates the high stability of the J-aggregated form of PIC-closo-hydrodecaborate. For example, the addition of octadecyl choline iodide to films of PIC iodide with long alkyl substituters ($C_{18}H_{37}$) leads to the decomposition of the J-aggregates to the monomer at a dye–additive mole ratio even as low

as 1 : 0.1. In fact, at a concentration of the additive organic cation at 4 times higher than the concentration of the dye cation, the molecules of the organic salt of the additive cation can be considered as a kind of a matrix for the dye molecules.

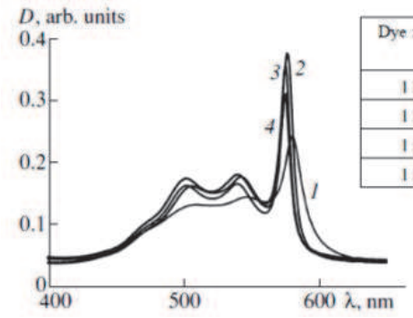

Dye : TBA	λ_{max}, nm	*J/M*	Full width at half maximum, cm^{-1}
1 : 0	580	1.66	585
1 : 2	576	2.14	326
1 : 4	575	2.15	271
1 : 5	575	1.68	289

Fig. 19. Absorption spectra of films of PIC-closo-hydrodecaborate doped with tetrabutylammonium iodide (the dye–additive mole ratios, maximum wavelengths of the J-peak, *J/M* ratios and the full widths of the peaks at half maximum are given in the inset). Spectra *1–4* correspond to the dye–additive mole ratio varied from 1 : 0 to 1 : 5, respectively

The dilution of a film of PIC-closo-hydrodecaborate with organic cations leads to an increase in the luminescence of J-aggregates. The luminescence spectra of the J-aggregates in a film of PIC-closo-hydrodecaborate and in an analogous film diluted with TBA cations in the ratio dye–TBA 1 : 4 measured under identical excitation conditions are shown in Fig. 20. It is seen from this figure that, upon dilution of the J-aggregated film by TBA cations, the luminescence intensity of the J-aggregates increases by an order of magnitude. This effect can be explained by a decrease in the concentration quenching of luminescence of the J-aggregates.

In our opinion, the changes in the shape of the J-peak in the absorption and luminescence spectra of thin films of PIC-closo-hydrodecaborate observed upon dilution of the films with foreign organic cation can be explained by the fact that this peak arises due to the absorption of strongly coupled PIC dimers. A stable dye dimer may form because of a strong electrostatic interaction of two cationic molecules PIC+ with a doubly charged polyhedral $B_{10}H_{10}^{2-}$ anion. In a dimer PIC_2-$B_{10}H_{10}$, the electrostatic interaction is saturated and, upon dilution with foreign cations, large-size aggregates should decompose.

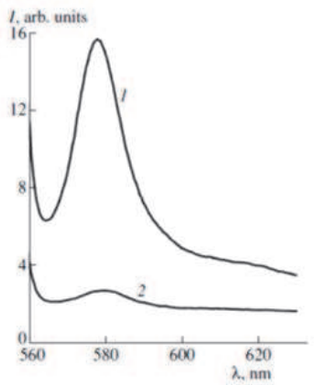

Fig. 20. Thin solid films luminescence spectra (*1*) PIC-closo-hydrodecaborate doped with TBA at a dye–TBA mole ratio of 1 : 4 and (*2*) pure PIC-closo-hydrodecaborate

The charge distributions in the dye cation and in the anions of the highest boron hydrides were calculated by the AM1 method and are shown on the structures below. Qualitatively, the calculated charge distribution among the atoms of the known anions $B_{10}H_{10}^{2-}$ and $B_{12}H_{12}^{2-}$ agrees with the charge distribution calculated by such methods as PRDDO, 3D Huckel theory and STO-3G (Pilling & Hawthorne, 1964). Quantitatively, the best agreement was obtained for the total charges of the B–H groups.

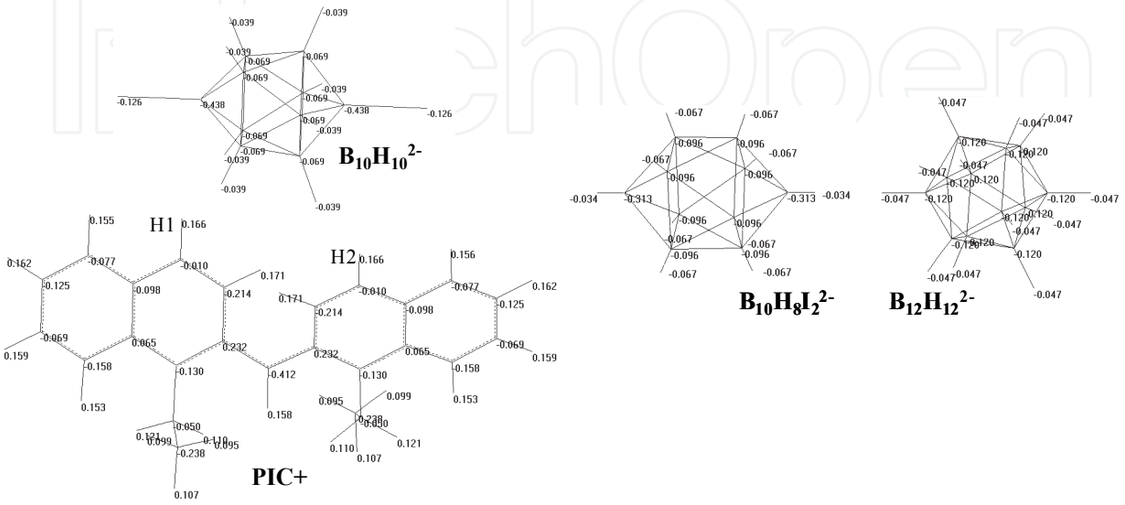

In the $B_{10}H_{10}^{2-}$ anion, a negative charge is distributed non-uniformly. The vertex B–H groups carry a larger negative charge (–0.347) than the equatorial B–H groups (–0.163). In the PIC cation, a highest positive charge is located on two carbon atoms of the heteroaromatic rings involved in the chain of conjugation. The remaining carbon atoms and nitrogen heteroatoms carry negative charges. The remaining positive charge is mainly distributed over the hydrogen atoms of the aromatic rings. The basic atomic centres of the electrostatic attraction of the ions considered are the vertex B–H groups in the $B_{10}H_{10}^{2-}$ anion, the carbon atoms and the hydrogen atoms of the heteroaromatic rings of the dye cation. The geometrical dimensions of the $B_{10}H_{10}^{2-}$ anion (the distance between the polar hydrogen atoms is equal to (5.9 Å)) correspond well to the dimension of the cavity of the electrostatic potential of PIC due to the turn of its aromatic planes, in particular, the distance between the positively charged hydrogen atoms H1 and H2 (5.6 Å). It should be noted that the involvement of the vertex B–H groups of the $B_{10}H_{10}^{2-}$ anion into the formation of a stable PIC-closo-hydrodecaborate complex is confirmed by the data of IR spectroscopy and x-ray diffraction analysis (Cerasimova, 2000). The structure of a dimer of PIC-closo-hydrodecaborate calculated using the MM+ method and the map of the electrostatic potential calculated using the semi-empirical quantum-chemical AM1 method are shown in Fig. 21. It is seen that the aromatic planes of the dye cations interacting via the anion of closo-hydrodecaborate are turned with respect to each other. This turn can be explained by the mutual repulsion of the positively charged aromatic hydrogen atoms in the PIC dimer.

The charge distribution in the $B_{10}H_8I_2^{2-}$ anion is more polarized than in the $B_{10}H_{10}^{2-}$ anion. The negative charge is strongly displaced toward the vertex boron and iodine atoms. If one assumes that the dipole charge distribution in the $B_{10}H_{10}^{2-}$ anion facilitates the formation of J-aggregates of PIC, then, upon addition of $B_{10}H_8I_2^{2-}$ anions, efficient J-aggregation should

also be observed. This agrees with the formation of J-aggregates of PIC in the presence of these anions in the case of the solution being held prior to its centrifugation for a time period longer than 10 min (Fig. 18). Upon deposition of a dye solution immediately after the addition of anion, an intensive association of the dye is likely to occur, which is stimulated by a relatively high initial concentration of anions localized near the drop of salt addition (later, the associates gradually dissolve). In this case, the intensive association of the dye leads to the formation of a set of strongly aggregated dimers of PIC, whose absorption extends toward the long wavelength range up to 800 nm. The maximum of this distribution (625 nm) possibly corresponds to the dye tetramers.

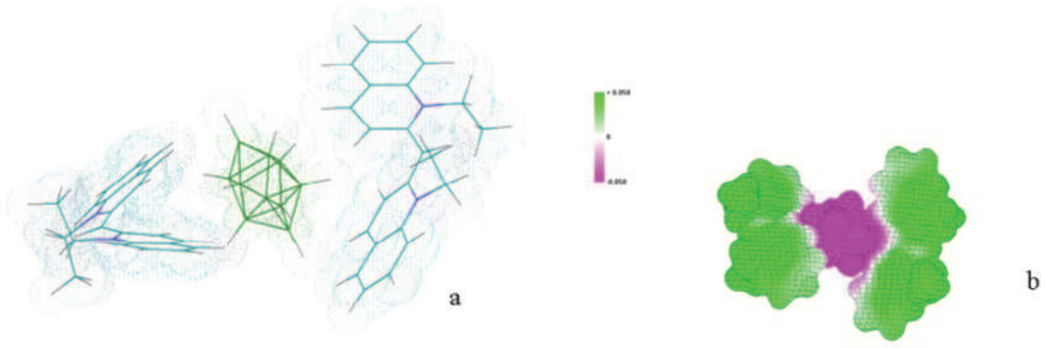

Fig. 21. The calculated structure of the PIC-closo-hydrodecaborate dimer (a) and dimer electrostatic potential map (b).

In the $B_{12}H_{12}^{2-}$ anion, the charge distribution among the boron atoms is completely uniform and the absolute value of the charge of the B–H groups (–0.167) is significantly smaller than that of the vertex B–H groups of the $B_{10}H_{10}^{2-}$ anion. Note that this anion has no poles of concentration of a negative charge and, therefore, no structure-forming effect on the formation of J-aggregates of PIC. Taking into account the charge distribution pattern in the considered cluster anions of boron hydrides, as well as their relative dimensions, we can conclude that a more pronounced bipolar distribution of the negative charge and a smaller volume of an anion facilitate the formation of a J-aggregate of PIC.

In the case of a strongly bound dimeric form of PIC-closo-hydrodecaborate, the dissociation of these dimers to the monomer upon dilution of dye films with a salt of an organic cation does not occur immediately, but rather via the stage of formation of separated dimers of PIC. The weakening of the intermolecular interaction leads to (i) a narrowing of the absorption peak of a J-aggregate, (ii) an increase in the intensity of the J-peak, (iii) a hypsochromic shift of the J-peak and (iv) an increase in the intensity of luminescence of the J-aggregate. We assume that the dimer of a dye is the main structural unit responsible for the absorption of a J-aggregate (J-peak) of PIC.

2.8 The thermal stability of PIC-closo-hexahydrodecaborate in the thin solid films

The thermal stability of the J-aggregates of PIC with long alkyl substituters in the thin solid films (T_{decay} about 60° C) is near the temperature of the film heating at pulse laser excitation. The laser destruction of these films takes place at laser intensity I_0=1-5 MW/cm². The film temperature change (ΔT) at the named intensity is 20-90° C from the equation:

$$\Delta T = \frac{I_0(1\text{-}10^{-D})\cdot(1\text{-}R)\cdot\tau}{h\cdot\rho\cdot C_p} \tag{18}$$

where, ρ - density 1,4 g/cm^3, C_p – specific heat capacity 3,1 J/g·K^0, D – film optical density 0,5, R – reflection coefficient 0,3, laser pulse duration τ=5ns, film thickness h=30nm.

The J-aggregates of PIC-closo-hexahydrodecaborate in the thin solid films are more suitable for the non-linear laser experiments due to their higher thermal stability compared with that for the J-aggregates of long chain PIC.

The thermal stability of PIC-closo-hexahydrodecaborate with TBA addition in solid films is studied by using the spectrophotometry method. The J-aggregates of PIC-closo-hexahydrodecaborate are stable at sample heating to temperature 90^{0}C and being partially destructed at higher temperature are restored to 100% at sample cooling to room temperature. As an example the thermal decay and restoring of the J-aggregates' PIC-$B_{10}H_{10}$ the spectral change of the J-aggregated film with addition of the TBA for peak narrowing is shown in the fig. 22 a. One of the features of the thermal decay of the J-aggregates' PIC in the thin solid films is the red shift of J-aggregate peak. An example of an evident red shift of absorption peak of J-aggregates is shown in fig. 22 b,c.

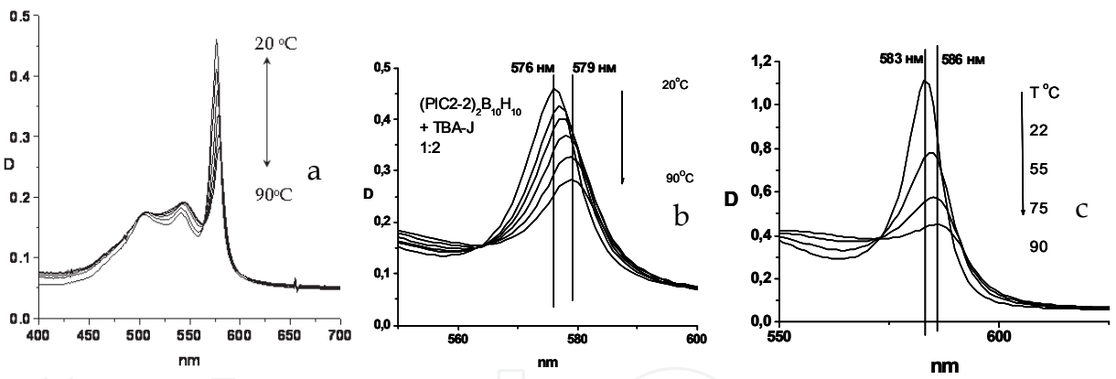

Fig. 22. The absorption spectra change of the J-aggregated films' PIC-closo-hydrodecaborate headed (cooled), doped with TBA at a dye–TBA mole ratio of 1 : 4 (a), expanded scale (b), expanded scale PIC2-2 in polymer anethole (c)

The red shift of the J-aggregate peak in thin solid films and polymer matrix to about 3 nm was observed in the causes of J-aggregates' thermal decay. This effect we connect with the inhomogeneous broadening of the J-aggregate absorption band. The red spectral shift caused by intermolecular interaction follows the depth of the J-aggregate potential in the ground state for the homogeneous absorption profile as it is considered for the positive solvatochromic shifts of the absorption spectra of the molecules (Suppan, 1990). The thermal decomposition takes place for local aggregates having different activation energy. The activation energy has inhomogeneous Gaussian distribution between J-aggregates sites with homogeneous spectral Lorentz profiles. In this case, each homogeneous Lorentz profile has the spectral position with proper own activation energy of thermal decay from aggregate

(dimer) to monomer. At the sample heating the aggregates with lower activation energy (ΔE_1) have a higher probability to destroy and have higher excitation energy. The inhomogeneous distribution of J-aggregates leads to spectral-kinetic non-equivalence of the thermal decay. The statistic weight of J-aggregates with high energy of activation increases during thermal decay.The combination of inhomogeneous broadening of initial homogeneous spectral Lorentz profiles of absorbing aggregates gives the Voight function (V) of spectral distribution.

$$V = 2\ln(2)\frac{\gamma}{\Delta w^2}\cdot\int_{-\infty}^{\infty}\frac{e^{-t^2}dt}{\left(2\ln(2)\cdot\frac{w-w_0}{\Delta w}-t\right)^2+\left(\ln(2)\frac{\gamma}{\Delta w}\right)^2} \tag{19}$$

Where, γ – width of Lorentz profile, w - width of Gauss profile and w_o – central position of absorption band. To take into account the individual rate of thermal decomposition of absorbing Lorentz profiles of aggregates, we need to include in the Voight function the equation describing the thermal decay curve, depending on the energy activation distribution. The equation for thermal decomposition as follows from (4) shown in the above curve is

$$\begin{gathered}1-\alpha_T=\exp\left(-F_a\right)\\ F_a=\left[\frac{T^2R}{\Delta E_a}\cdot\left(1-\frac{2TR}{\Delta E_a}\right)\cdot\exp\left(-\frac{\Delta E_a}{TR}\right)\right]\cdot Z\end{gathered} \tag{20}$$

Where, α_T is the degree of J-peak decay, T – temperature ^{o}K, R – universal gas constant, Z – preexponential factor Z=10^{18} and ΔE_a – activation energy with average value 120 kJ/mol. The values correspond to the thermal decomposition behaviour of J-aggregates' peak for PIC2-15 in thin films. We suppose that the activation energy spectral distribution has the normal distribution profile in spectral region of J-aggregate absorption with deviation ±10 kJ/mol**.** The Voight function, including the degree of thermal decomposition $V(E_a,T)$, is

$$V(E_a,T)=2\ln 2\cdot\frac{\gamma}{\Delta w^2}\int_{-\infty}^{\infty}\frac{e^{-t^2}\cdot e^{-F_a}}{(2\ln 2\frac{w-w0}{\Delta w}-t)^2+(\ln(2)\cdot\frac{\gamma}{\Delta w})^2}dt \tag{21}$$

Calculation of the Voight contour of J-peak absorption was carried out. The values of homogeneous and inhomogeneous broadening of the J-peak are approximately equal and make up 235 cm^{-1} at room temperature. The results of modelling of the Voight contour of J-aggregate PIC2-15 absorption at the stage of thermal decomposition was compared with the experimental spectral curves of J-aggregate (see fig. 23).

One can see good agreement between modelling and experimental spectral curves. The results confirm the influence the inhomogeneous broadening of absorption spectra of J-aggregates in thin films on the red shift of absorption band of J-aggregates at thermal decay.

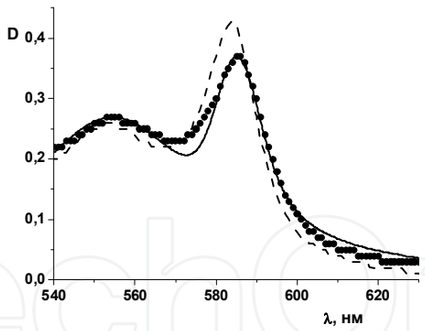

Fig. 23. Calculated Voight contour of J-aggregates at 55°C (solid lines) and experimental absorption curves of thin solid films of J-aggregates of PIC2-15: dash curve - initial spectrum, dot curve - spectrum at 55°C

2.9 The spectrophotometry of J-aggregate thin film formation by spin-coating

Thin film formation of J-aggregated pseudoisocyanine iodide with long alkyl substituents PIC 2-18 and PIC 2-2 with the addition of $B_{10}H_{10}^{2-}$ anion was studied by spectrophotometry directly during spin-coating of the dye solutions. The view of spectra change during spin-coating of a solution of PIC 2-18 at 2000 rpm from the time of placing the solution until formation of the solid J-aggregated film is shown in Fig. 24. The inset shows the change of optical density at the absorption maximum of the monomer form of dye Fig. 24a. The initial spectrum of dye solution on the substrate exhibits optical density noise fluctuations because it exceeds the dynamic range of the spectrophotometer (2.5*D*). After 2.5 sec from the spin-coating stars, the dye absorption in solution stabilizes at optical density *D*=1.3 and remains unchanged for 0.4 sec. This means that the centrifugal discharge of dye solution from the substrate is finished and the film is held on the substrate by surface-tension forces. The dye concentration increases because of solvent evaporation from the thin film, whereas the number of dye molecules on the substrate remains the same. Fig. 24b shows the spectral changes for a film of PIC 2-2 (+$K_2B_{10}H_{10}$) at rotation rate 1500 rpm. The time for formation of J-aggregates on substrate is 0.45 sec.

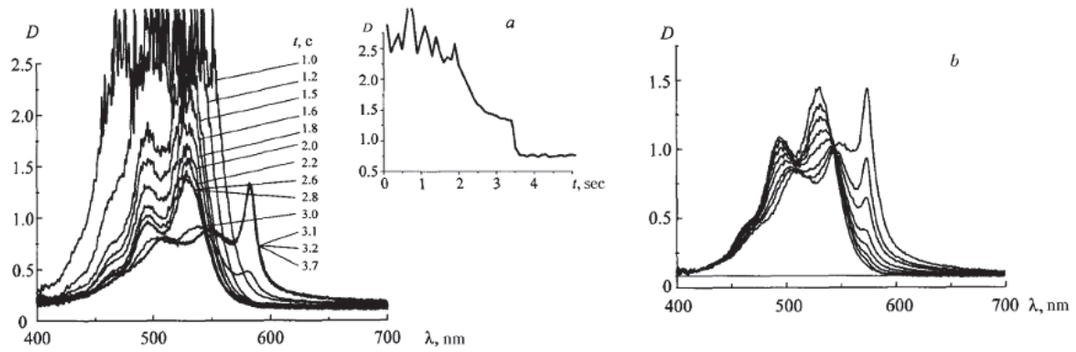

Fig. 24. Spectral changes during spin-coating of solutions of pseudoisocyanine derivatives: PIC 2-18 solution [the time from the moment of placing the solution on the centrifuge is shown; in the inset, optical density at the absorption maximum of the monomeric dye in solution (530 nm) as a function of spin-coating time] (a); PIC 2-2 solution with added $K_2B_{10}H_{10}$ during formation of J-aggregate (spectra recorded every 0.05 sec) (b).

It should be noted that the experimental spectra are not corrected for double passage of light through the sample. Losses of light to double reflection and absorption of dye film must be considered in order to obtain the true value of the optical density in our optical setup. For this, the reflectance spectrum of J-aggregated PIC 2-18 film was measured (Fig. 25). The corrected optical density of J-aggregated film $D(\lambda_{cor})=\log [I_0/(I_0-A-R)]$ was calculated by solving the quadratic equation for the absorption coefficient obtained from the formula for the measured optical density $D(\lambda)$:

$$10^{D(\lambda)}=\frac{I_0}{I_0-A-R-R\left(I_0-A-R\right)\left(I_0-A-R\right)},$$
$$A^2-A\left(1-2R+I_0\right)-\left(\frac{I_0}{10^{D(\lambda)}}-I_0+R+RI_0-R\right)=0. \tag{22}$$

where A is the absorption coefficient and R the film reflectance coefficient for each wavelength.

A comparison of Fig. 24 and Fig. 25 shows that correction of the spectrum taking into account double absorption and reflection decreases significantly the optical density of the sample at the maximum of the J-peak (to 0.3).

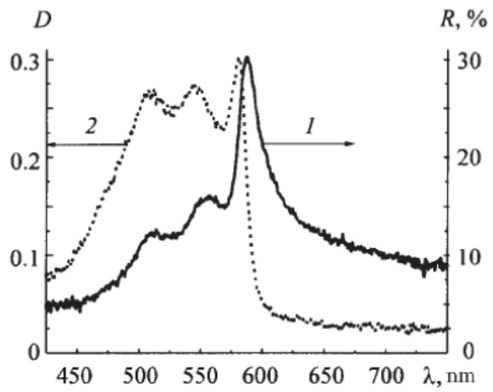

Fig. 25. Reflectance spectrum (1) and absorption spectrum calculated taking into account reflectance of the sample (2), J-aggregated film of PIC 2-18

Spectral changes occurring during spin-coating of J-aggregated PIC dye are related to the increased refractive index of the medium at the time of film formation. The bathochromic shift of the monomer dye absorption maximum is due to solvent evaporation and replacement of the initial medium with refractive index n_1, consisting of solvent molecules, by a medium with refractive index $n2$, consisting of dye molecules themselves. The absorption maximum of the dye for PIC film ($+B_{10}H_{10}^{2-}$) shifts from 529 to 550 nm as the film dries out; for PIC 2-18 film, from 529 to 551 nm. The spectral shift in organic molecules on going from vacuum to a medium with refractive index n_0 is described by the universal interaction function (Bakhshiev et al., 1989)

$$\Delta v=\text{const}\cdot\frac{n_0^2-1}{n_0^2+2} \tag{23}$$

An empirical expression for the universal interaction function of dye with medium was obtained based on experimental data for absorption of PIC monomer in various media (Renge & Wild 1997)

$$\lambda(n_0) = \frac{10^7}{19716 - 2964\left[\left(n_0^2 - 1\right)/\left(n_0^2 + 2\right)\right]} \tag{24}$$

where $\lambda(n_0)$ is the wavelength (nm) of the absorption maximum for dye in a medium with refractive index n_0.

The refractive index of the medium for dye solution is n_m=1.405. The wavelength of the absorption maximum of monomer dye λmax=526.6 nm was calculated using Eq. (24) and agrees with the experimental value for a dilute dye solution. The refractive index of film after centrifugal discharge of dye solution from the substrate obtained using Eq. (24) was 1.47 for absorption of PIC monomer at 529 nm. From this point the spectral shift of the absorption band of dye monomer during spin-coating from 529 nm to 551 nm corresponds to a transition from a medium with refractive index n=1.47 to a medium with n=2.1. That is in agreement with n value from the dispersion curve for dye in thin film (see fig. 12a).

Thus, the bathochromic shift of the dye absorption spectrum at the time of film formation is due to the increased polarizability of the medium. Therefore, the polarization spectral shift must be considered in determining the exciton splitting of the monomer absorption band upon J-aggregation or the energy of exciton coupling of dye molecules in the J-aggregate (Jex). The experimental value Jex is determined from the energy difference of the long wavelength transition of PIC in solution (530 nm) and in the J-aggregate using the formula (Kuhn & Kuhn 1996)

$$\Delta E = \sqrt{E_m^2 + 4E_m J_{ex}} - E_m \tag{25}$$

where, Em is the energy of the long wavelength transition in the monomer; Jex, the exciton coupling energy; and ΔE, the energy difference of absorption at the monomer peak and the J-peak. The absorption maximum of the J-peak was observed at λ=570 nm where the absorption of PIC J-aggregates was measured in aqueous ethyleneglycol matrix at liquid helium temperature (Minoshima et al., 1994). In this instance Jex=632 cm^{-1}. A similar value of Jex is used in theoretical calculations. In particular, Jex ≈ 600 cm^{-1} is used to determine the exciton delocalization length (Bakalis & Knoester, 2000).

The change of local field for a dye molecule in the aggregate as a result of the change of medium is not considered for this estimate of Jex. The total energy of the J-peak shift of aggregate absorption is the sum of the polarization energy and the exciton coupling energy of neighbouring molecules in the aggregate. Therefore, the bathochromic shift of the dye S_{00}-transition that is due to the medium polarizability with an effective refractive index equal to the refractive index of the dye monomer in the solid phase, i.e., n=2.1, must be taken into account for dye molecules in the aggregate. The exciton coupling energy is Jex=293 cm^{-1} for the spectral maximum of monomer absorption shifted to 555 nm and for the absorption maximum of the J-peak located at 574 nm. Thus, the resulting value Jex ≈ 300 cm^{-1} is half of that used in the literature (Jex ≈ 600 cm^{-1}). The values Jex for aggregates of other dyes,

known from the literature (Moll, 1995), are also estimated based on the spectral shift of the absorption maximum of J-aggregated dye relative to the monomer in solution. The polarization spectral shift for dyes with highly polarizable π-electrons is significant. This correction must be considered in estimating *J*ex, not only for PIC aggregates, but also for aggregates of any other dyes.

Another aspect of the change the local field factor at the J-aggregate formation is the dramatic increase of the J-peak at the last moment of formation of the solid film without a decrease of the optical density at the absorption maximum of the monomeric dye, i.e., the significant growth of the optical density of the J-peak is not compensated by a decrease of the monomer optical density. An additional increase of the J-peak, for example, for PIC 2-2 ($+K_2B_{10}H_{10}$) by 2.15 times can be seen from the measured absorption spectra.

One reason for the increased absorption as the film dries out is the increased refractive index of the medium. According to Bakhshiev et al. (1989), the ratio of integrals of absorption intensity (Int) in media with different polarizabilities (Int_{max} for n_{max} and Int_{min} for n_{min}) depends on the local field factor

$$\frac{\mathrm{Int}_{\max}}{\mathrm{Int}_{\min}} = \frac{\left(n_{\max}^2+2\right)^2}{9n_{\max}} \frac{9n_{\min}}{\left(n_{\min}^2+2\right)^2} \tag{26}$$

The monomer concentration ceases to decrease with a spectral shift of the monomer peak to 539 nm. According to Eq. (24), the refractive index of the medium at this moment n=1.7. The ratio of local field factors is 1.94 for a change of medium refractive index from 1.7 to 2.5. The calculation in the optical density change, taking into account the reflection and absorption growth due to growth of the local field factor, gives the increasing measured optical density of the J-peak by 2.2 times and explains the increase of the J-peak without loss of dye monomer.

The results from the investigation of J-aggregate formation during spin-coating of PIC indicate that the change of local field factor should be considered in interpreting spectral properties of nano-structured aggregates for any type of dye aggregation or for other highly polarizable molecules in both films and solutions.

2.10 The third order non-linear optical properties of pseudoisocyanine J-aggregates in thin solid films

The third order non-linear optical properties of pseudoisocyanine J-aggregates in thin solid films were studied using the Z-scan method as well for PIC iodide anion as for PIC with closo-hexahydrodecaborate anion ($B_{10}H_{10}^{2-}$) (Markov et al., 1998a, 1998b; Plekhanov et al., 1998a, 1998b). The dispersions values of imaginary $Im\chi^{(3)}$ and real $Re\chi^{(3)}$ parts of cubic susceptibility of J-aggregated film are shown in fig. 26. In both causes the non-linear bleaching of the solid film samples in J-peak maximum is observed at resonance laser irradiation excitation ($I>10^5$ W/cm^2) and obvious darkening on the red side of the dispersion curve of imaginary part of $\chi^{(3)}$. J-aggregates of both types of dye have a similar value of the coefficient of non-linear absorption $\beta \approx -6*10^{-2}$ cm/W and corresponding value $Im\chi^{(3)} \approx -1*10^{-5}$ esu at the bleaching maximum and $Im\chi^{(3)} \approx 0.12*10^{-5}$ esu at the maximum of

darkening. At the intensity of the laser irradiation at more than 3 MW/cm², the films become irreversibly burned.

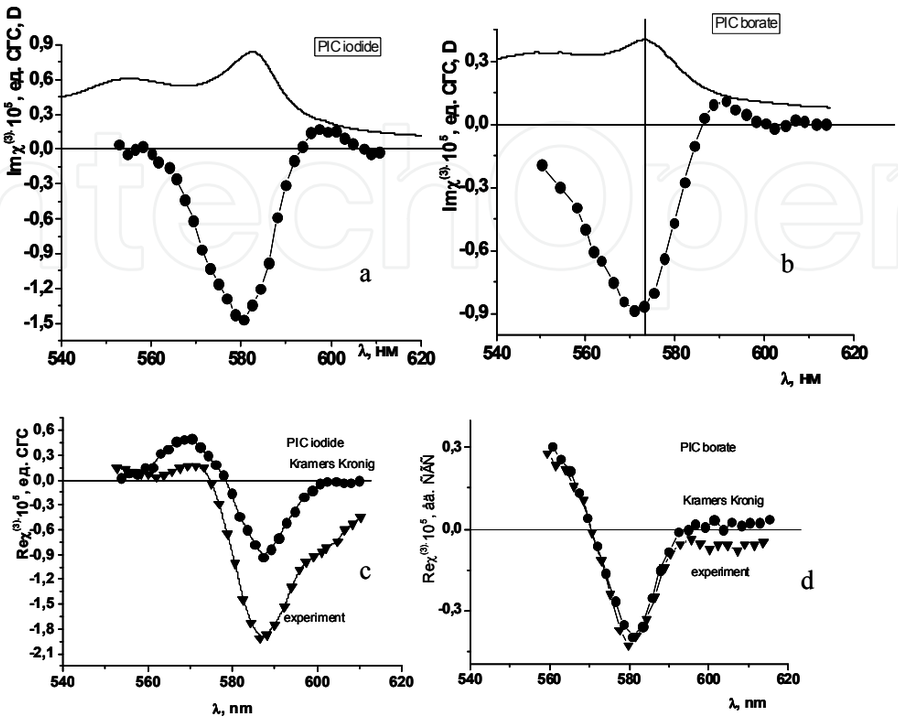

Fig. 26. a-d. The dispersion curves of the imaginary part of the cubic susceptibility of the J-aggregated $Im\chi^{(3)}$ PIC-iodide (a) and closo-hexahydrodecaborate (b) and real $Re\chi^{(3)}$ PIC-iodide (c) and closo-hexahydrodecaborate (d) compared with Kramers-Kronig calculated curves

The maximal value of the real part of the cubic susceptibility for films with J-aggregate of PIC-iodide is $Re\chi^{(3)}$=-1,8*10^{-5} esu and with J-aggregate of PIC-closo-hexahydrodecaborate $Re\chi^{(3)}$=-0,45*10^{-5} esu. This difference is due to the contribution of the refraction thermal change in the higher absorption PIC-iodide film compared with absorption of PIC-($B_{10}H_{10}^{2-}$) film as is shown in fig. 27. The imaginary part of the cubic susceptibility does not depend on the thermal contribution. The sample refraction change caused by saturation of the electron transition without the part of thermal contribution was calculated by Kramers-Kronig relation connecting the $Im\chi^{(3)}$ and $Re\chi^{(3)}$ for the non-linear case (Markov et al., 1998c) (see fig. 26 a-d).

$$\mathrm{Re}\,\chi(\Omega) = \frac{1}{\pi}\int_{-\infty}^{\infty}\frac{\mathrm{Im}\,\chi(\Omega)}{x-\Omega}dx - 2\,\mathrm{Re}[C^{-1}{}_{(\Omega_p)}(\Omega)] \qquad (27)$$

where C^{-1} is the residue in the pole of the $\chi(\Omega)/x-\Omega$, ($\Omega=\omega-\omega_l$) function.

The thermal contribution to the non-linear refraction for the films with the optical density D<0.4 is insignificant, but it should be considered for films with optical density D≈1. The maximal values of the real parts of $\chi^{(3)}$ with and without taking into account the thermal

contribution are close to each other and are $Re\chi^{(3)} \sim -(0.5\text{-}0,7)*10^{-5}$ esu. The obtained values of the non-linear response of PIC J-aggregates in the thin solid films ($\chi^{(3)} \approx 10^{-5}$ esu) are two orders of magnitude higher than in the water solution (Bogdanov et al., 1991) and polymer matrixes (Plekhanov et al., 1995) ($\chi^{(3)} \approx 10^{-7}$ esu). Apart from the much lower values of the cubic susceptibility, there was no observation of non-linear darkening of PIC J-aggregates.

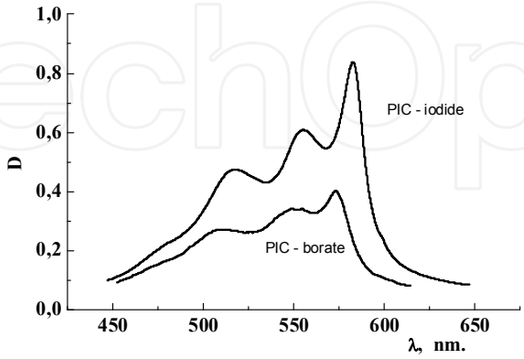

Fig. 27. The absorption spectra of the PIC2-2 iodide and closo-hexahydrodecaborate J-aggregated films

The iodine anion existing in the PIC molecule has the high polarizability and the more the iodine atoms are in the anion molecule, the higher the polarizability. The PIC J-aggregated film with addition of high polarizability tetraethylammonium salt of the closo-tetrahydrohexaiodo-dodecaborate ($B_{10}H_4I_6^{2-}(C_4H_9)_4N^+$) which has six iodine atoms was prepared to raise the J-aggregate surrounding polarizability. The dispersion curve of the imaginary part of the obtained film is shown in fig. 28 compared with the dispersion for the PIC-closo-hexahydrodecaborate film.

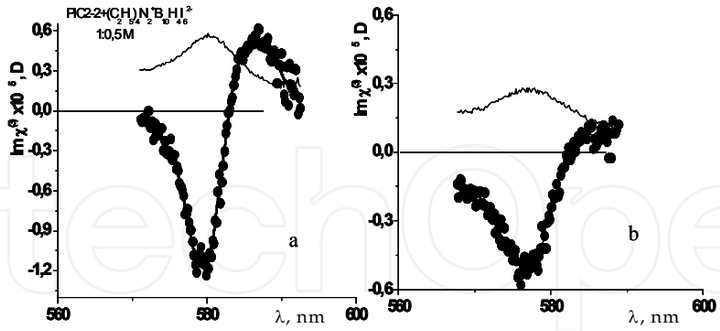

Fig. 28. The cubic susceptibility dispersion curves for the PIC J-aggregated films with - $B_{10}H_4I_6^{2-}$ 1:0,5 (a) and $B_{10}H_{10}^{2-}$ 1:0,5 (b)

As one can see from the adducing figures, the non-linear optical response of the J-aggregated film samples with high polarizable anion ($B_{10}H_4I_6^{2-}$) is higher than for the film with $B_{10}H_{10}^{2-}$ anion. The negative value of the imaginary part of the cubic susceptibility increases 2 times and the red shifted induced non-linear absorption increases in 5 times up to $0.6 \cdot 10^{-5}$ esu. That means it is possible to act upon the non-linear response of the charged aggregated molecules by additions of the proper anions.

The non-linear darkening on the red side of dispersion $Im\chi^{(3)}$ curves is considered on the basis of the four-level model of excitation energy relaxation in PIC J-aggregates shown in fig. 29. The additional level of the relaxation of the first singlet state of J-aggregates in the thin film arises from high polarization of the surrounding J-aggregate medium consisting of the PIC dye molecules. The equations obtained in (Tikhonov & Shpak, 1977) for a four-level model of the excitation relaxation in assumption $k_4 >> k_2$ were used to calculate the induced bleaching and darkening change in the J-aggregated thin film depending on the intensity of the incident laser radiation.

$$\Delta T = \frac{1 + \frac{I_0\sigma_{32}}{A_k}\cdot\left(\frac{1}{\tau_2} - \frac{\sigma_{10}}{\tau_3\sigma_{32}}\right)}{1 + \frac{1}{A_k}\cdot\left[\sigma_{10}I_0\left(\frac{1}{\tau_2}+\frac{1}{\tau_3}\right) + \sigma_{10}\sigma_{32}I_0^2\right]} - 1 \qquad (28)$$

$$A_k = \left(\frac{1}{\tau_1}+\frac{1}{\tau_2}\right)\cdot\left(\frac{1}{\tau_3}+\sigma_{32}I_0\right) \qquad \sigma = \frac{2303\cdot\varepsilon}{6.02\cdot10^{23}}$$

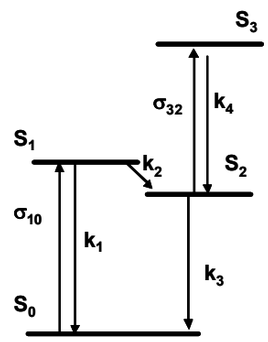

Fig. 29. Four-level model of the J-aggregate excitation relaxation in thin film, where, S_2 excited state is considered here as relaxed S_1 state

The luminescence kinetics decay for J-aggregated film was measured to estimate the values of the characteristic times of excited state relaxation. The luminescence decay of the J-aggregated thin film in the maximum of the J-aggregate luminescence λ=590 nm at the excitation in J-peak maximum λ=574 nm at temperature 94^0K is shown in fig. 30.

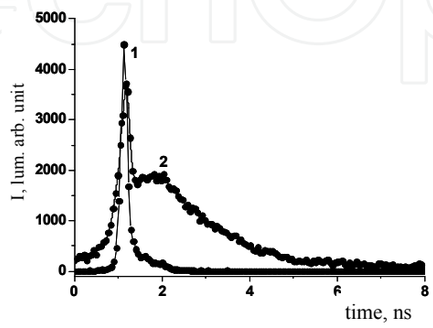

Fig. 30. Signal instrument function (1) and decay kinetics luminescence curve J-aggregates PIC2-15 in the film (2) excitation λ=574 nm measurement at 590 nm,T=96^{o}K

The fast and slow components of the luminescence decay take place on the luminescent decay kinetic curve. The signal instrument function was 80 ps. The expanding of the instrument function due to the appearance of the fast component is 20-40 ps. The life time of the slow component is 2 ns. The period of the luminescence growth of the slow component takes place with characteristic time 0.1-0.2 ns. The existence of the fast and slow components is typical for the dye molecules in polar liquid and solid phases. Some relaxations times from picoseconds to nanoseconds relate to different processes of the solvate shell relaxation depending on the characteristic times of the anionic and cationic parts of the medium relaxation in the case of organic or inorganic salts (Ferrante et al., 1998; Saha et al., 2004; Das et al., 1996; Mandal et al., 2002; Arzhantsev et al., 2003). The luminescence of the J-aggregate in the thin solid film occurs from the two states: the state of the fast matrix relaxation and state of the slow matrix relaxation which is populated in a time of about 100 ps. Different luminescent life times 20-40 ps, 128, 659 пс, 1.7 нс were reported depending on the preparation condition and irradiation intensity (Sundstrom et al., 1988) for the PIC J-aggregates in solvents.

The initial values of the parameters of the model are determined as: J-aggregate extinction coefficient ε_{10}=2 10^5 $M^{-1}см^{-1}$, the same value for S_2-S_3 transition ε_{32}=2 10^5 $M^{-1}см^{-1}$, τ_2=100 ps (from the time of the slow component luminescence increasing), τ_3=2 10^{-9}s (the life time of the luminescence decay slow component), τ_1=10^{-11}s is a typical value of the non-radiation relaxation in organic molecules, the relation of the width values of the transition $S_{1\text{-}0}$ and $S_{3\text{-}2}$ spectral contours was taken from measurement of dispersion of the non-linear bleaching and darkening as 150 and 120cm^{-1}. The model describing the dispersion of the induced transmission in the non-linear experiment is composed by including into eq. (28) the value of the $\sigma_\lambda(\varepsilon)$ for the transition $S_{1\text{-}0}$ and $S_{3\text{-}2}$ in the form of the Lorentz contour $\sigma_\lambda = \sigma_0 \cdot \Delta\upsilon^2 / 4 \cdot (\upsilon - \upsilon_0) + \Delta\upsilon^2$.

The model curve (the red curve in fig. 31a) is close to the experimental curve. The moderate change in the relaxation time $\mathbf{S}_1$ level to $\mathbf{S}_2$ level from 100 ps to 150 ps leads to the well fitting of the model (blue curve) and experimental curves. The shift of the maximum of the non-linear absorption (λ=580 nm) from the maximum of the non-linear transmission (λ=575 nm) on the 150 cm^{-1} follows from the calculation. It corresponds to the shift of the luminescence maximum relative to the absorption maximum of the J-aggregates in the thin solid films.

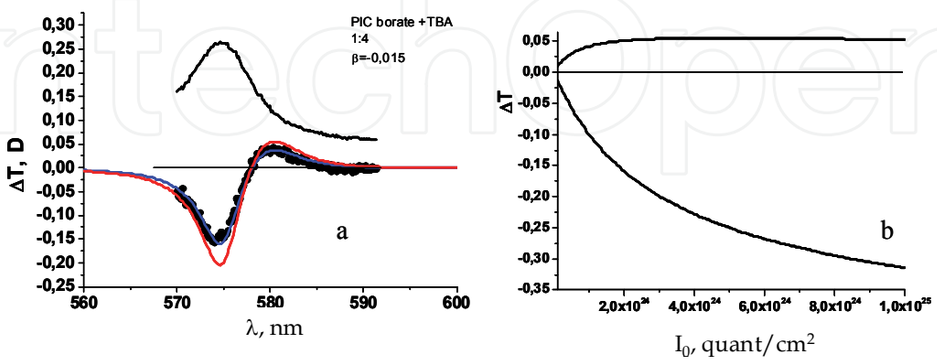

Fig. 31. The calculated (blue and red curves) and experimental (points) non-linear transmission dispersion curves for the J-aggregated PIC ($B_{10}H_{10}^{2-}$)+TBA (1:4) film (a); The calculated induced absorption (upper curve) and transmission (bottom curve) depending on the intensity laser irradiation (b)

The laser radiation intensity dependence on the non-linear transmission of the J-aggregated film sample was calculated for the obtained specified model parameters for the intensity change in the range 10^{23}-10^{25} quant/cm^2 in the maximums of the induced non-linear bleaching and darkening as shown in fig. 31b.

The experimental values of the induced darkening (ΔT=-0.05) and bleaching (ΔT=-0.2) are in good agreement with the calculated values at the experimental achieved intensities 10^6 W/cm^2 ($3 \cdot 10^{24}$ quant/cm^2). The calculated curves also coincide well with the existence of the experimentally observed saturation, as well in induced bleaching as in the induced darkening. At intensity of laser irradiation of more then $2*10^6$ W/cm^2 ($6 \cdot 10^{24}$ quant/cm^2) the irreversible burning of the dye film begins and observation of the non-linear effect becomes difficult.

Using the four-level model for J-aggregates appearing from the polarization relaxation of J-aggregate excites state is closely connected with the inhomogeneous broadening of J-aggregate absorption and luminescence spectrum, and can help us to explain the giant cubic non-linear properties of PIC J-aggregates in thin films. The big resonance values of the cubic susceptibility at the level $\chi^{(3)}=10^{-7}$ esu observed in the water solutions or in the polymer matrixes at high relation polymer:dye (>10:1) are caused by the high oscillator strength of the resonance transition in two level system (Zhuravlev et al., 1992; Shelkovnikov et al., 1993). The J-aggregate in the water is surrounded by weak polarizable water molecules and the excitation-induced medium polarization has a weak influence on the change of the energy of the excited electron level of the aggregate. The non-linear response in this case is the response of the two-level system. In the solid film the J-aggregate is surrounded by highly polarizable molecules of the dye. In this case induced medium polarization leads to the deep relaxation of the energy of the excited $\mathbf{S}_1$ level of J-aggregate to the relaxed state with the energy lowering to 150-170cm^{-1}. This process lasts 150 ps and in the laser pulse duration time 5 ns the effective population of the relaxed level takes place. This effect has the reflection in the linear spectrum as the inhomogeneous broadening of the absorption and luminescence contours of the J-aggregates in films. The decreasing of the population non-relaxed $\mathbf{S}_1$ level leads to the essential non-linear bleaching of the J-aggregates and to the appearance of the giant non-linear susceptibility of the J-aggregates. The excitation of the populated relaxed level leads to the appearance non-linear darkening at the long wavelength slope of the J-peak in solid films. The non-linear response of the J-aggregates in the solid films is the response of the four-level system and this leads to the increasing cubic susceptibility by two orders of magnitude. The additional reason of the non-linear response increasing in solid film is the increasing of the local field factor ($F_a = \frac{\left(n^2+2\right)^2}{9n}$) due to surrounding of the J-aggregate by highly polarizable molecules of the dye. The $\boldsymbol{F_a}$ is increased by 1.65 times at the transition from dye in the solvents to the dye in the film. The cubic susceptibility depends on the four degrees of the local field factor $\chi^{(3)} = \gamma \cdot F_a^{\,4} \cdot C$ (where C is the concentration, γ is the own polarizability of the molecule). This gives rise to the non-linear response up to seven times more.

2.11 The quantum chemical calculation of monomer and dimer PIC

The calculation of the charge distribution in the ground and excited state in the PIC2-2 molecule was carried out using the semi-empirical quantum chemical AM1 method. The charge distribution in the ground state of the cation PIC is shown in part 8 of this chapter. It coincides with the charge distribution calculated using the theory of the functional density method used in Guo et al. (2002) on the qualitative level. The charge redistribution on the atoms of the PIC molecule takes place at the excitation. Let take the transition dipole moment of the molecule be proportional to the electron density change at the excitation. The value of the electron density change between the ground and excited state was estimated by the change of the values of the dipole moments of the bounds between the neighbour atoms of the PIC π-system. The directions of the charge redistribution in the excited state of the PIC are shown in fig. 32a for one half of the molecule.

The redistribution of the electron density in the excited state of PIC leads to the next induced dipole moments in the molecule: the projection of the induced dipole moment along the X axe M_x=1.38D, along the Y axe M_y=1.44D. That means the total dipole induced by the electromagnetic field of the light wave is oscillated at the angle ~45^o in the XY plane of the molecule as shown in fig. 32b.

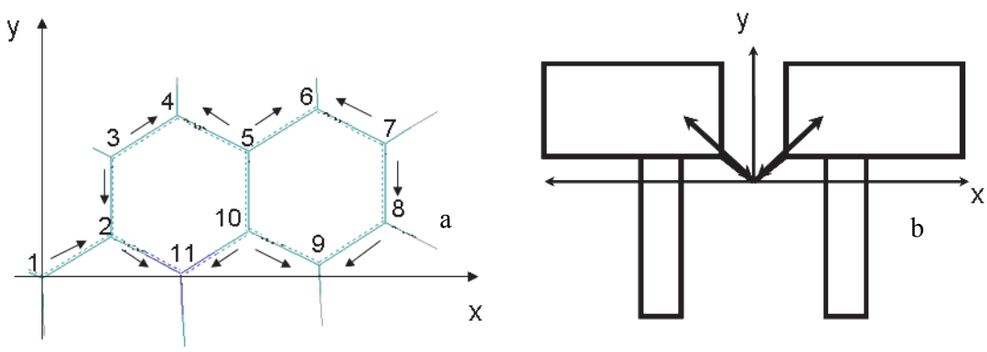

Fig. 32. The charge redistribution (a) and electron density oscillation at the PIC molecule excitation (b)

Since the directions of the projections of the induced dipoles vectors on the X axe are in opposition to each other, then only the induced dipoles vector projection directed along the Y axe is kept safe. It appears from this that the transition dipole moment is polarized along the short axis of PIC molecule.

The approximation of the dipole-dipole interaction between excited molecules in J-aggregate (Kuhn, H., Kuhn, C. 1996) does not consider the orbital overlap of the molecules. On the short distance between molecules in the aggregate, about 3-4 Å orbital overlap is essential. The existence of the orbital overlap between the neighbour dye molecules leads to the existence of the electron exchange between the orbitals and to the splitting of the electron levels of the two combined molecules. The exchange interaction has repulsive character for the system with closed shell as the dye in the ground state. This leads to the increase of energy of the two neighbour molecules in dimer. The excited state is the state with open shell and the dimer excitation takes place as as well to the high as to the low energy excited state. The energy of the splitting has the exponential decay dependence on

the distance and at the distance more than 10Å is about some inverse centimetres. But at the distance between molecules in dimer 3-4Å the energy of the splitting is hundreds of the inverse centimetres.

The splitting energy induced by exchanging orbital interaction is calculated via the resonance integral (β) distance dependence. The lowering of the energy of the transition is equal β and the value of the splitting is 2β. The excited state of the long wavelength transition of the PIC is $\pi-\pi^*$ excited state and it is reasonable to estimate the energy of the exchange interaction between molecules in dimer for the π–orbitals. For the estimation in the first approximation of the β value without application for the calculation of the advanced quantum-chemical methods it is possible to use the distance dependence of the resonance integral $\beta_{res}(r)$ given via calculation of the empiric integrals in the basis of the Slater-type orbitals for the π–orbitals of the conjugated double bounds in molecule that was cited in Warshell (1977).

$$\beta_{res}(r) := \left[2.438 \cdot e^{-2.035 \cdot (r-1.397)} \right] \cdot [\, 1 + 0.405 \cdot (r - 1.397)\,] \cdot 8065\,(cm^{-1}) \qquad (29)$$

The calculated value β_{res} for the distance 3,4-3,6 Å is 600-420 cm^{-1}. The estimated value β_{res} gives an image of the upper boundary of the lowering of the energy for two interacting $\pi-\pi$ orbitals because it was set for the orbitals in molecule. In the some of publication the short-range electron-exchange or electron/hole charge transfer between molecules was included in the calculation for the considering of the excited state of aromatic dimers as the exciton state, (Tretiak, 2000). It was shown that intermolecular electron exchange coherent interaction leads to a crucial red shift in the dimer spectrum and completely invalidates the simple Frenkel exciton model.

The splitting and oscillator strength of the PIC-dimer depend on the configuration of the interacting orbitals and thus the arrangement geometry of the dyes in the dimer. The energetic scheme of the electron levels splitting in the dimer is shown in fig. 33. The energy of singlet transitions in absorption spectrum of PIC in monomer form was calculated using the semi-empirical quantum chemical method ZINDO/S with preliminary geometry optimization utilizing the semi-empirical quantum chemical method AM1. The calculated PIC monomer structure in the model of the overlapping spheres is shown in fig. 34. The calculated long wavelength singlet transition at 509 nm with oscillator strength 1.3 is in accordance with the absorption of molecule PIC in a vacuum (calculation from the equation 24).

The calculations of energy of transitions in PIC dimers on the basis of the supramolecular approach using the semi-empirical quantum chemical method ZINDO/S with dimer geometry optimization utilizing the molecular mechanic method MM+ shows that the two-level splitting of the energy of excited state of dimer and magnitude of splitting depends on the angle between PIC molecules. It is significant that in the previous PIC dimer calculations (Kuhn & Kuhn, 1996; Burshtein et al., 1997) the linear shift of the molecules was considered. Here we consider the model of the molecules rotation in the PIC dimer. The calculation of the energy of the dimer by MM^+ method was accompanied by the optimization anion location at each step of the rotation equal to 5^o of the PIC1 molecule in ZX plane relative to the PIC2 molecule as shown in fig. 35. After the whole cycle of the rotation by 90^o, the distance L along the Y axe was changed and the cycle was repeated.

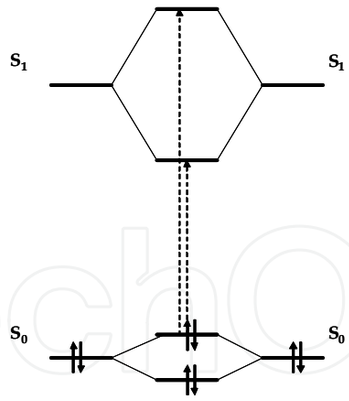

Fig. 33. The energetic scheme of the dimer levels splitting

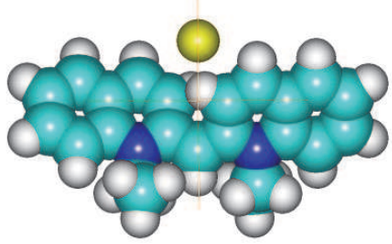

Fig. 34. The overlapping sphere model of the PIC iodide

The dimer energy distance (L) dependence for the three angles PIC molecules rotation perpendicular, parallel and at the angle of rotation 20° is shown in fig. 36. One can see that parallel molecules' orientation shows the weak energy distance dependence at the molecules' rapprochement to the 9.5Å. In further, the high energy growth in dimer takes place. The reciprocal rotation of the molecules on the 20° degree leads to clear energy distance dependence with the minimum at 7.7Å. The close energy minimum at 7.8Å has the dimer with the perpendicular molecular orientation.

The energy and oscillator strength of the PIC dimer at the rotation of the molecules divided on distance 7.8 Å were calculated using the ZINDO/S method, including 3 orbitals in configuration interactions (CI). The results of the calculation for two first allowed singlet transitions are shown in fig. 37.

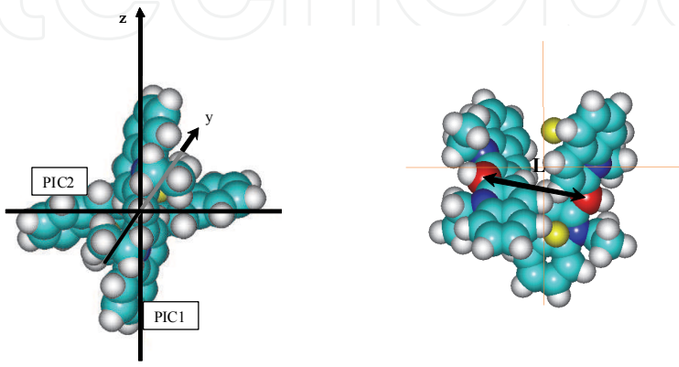

Fig. 35. The two profiles of the PIC molecules orientation in the dimer

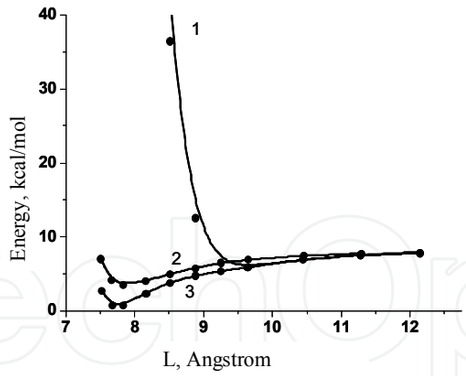

Fig. 36. The energy of the dimer molecular distance dependence for the three angles of the molecules rotation in ZX plane: 0° (1), 90° (2), 20° (3)

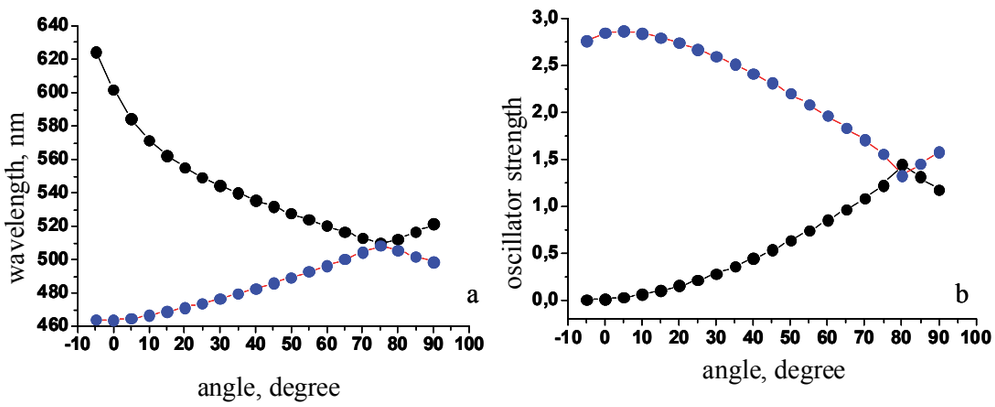

Fig. 37. The values of the wavelengths (a) and ascillator strength (b) for the two allowed singlet transitions in the PIC dimer depending on the rotation angle in ZX plane

The rotation of the dyes in dimer relative to axes connecting the centres of molecules leads to the splitting of the electronic levels giving the rise of the intensity of the short wavelength transition at parallel molecules orientation. That situation corresponds with appearance of the spectral absorption band of H-aggregates of PIC. At the angle between molecules of 75 degrees, which is close to a perpendicular orientation of the dye molecules, the energy level splitting becomes close to zero leading to the degeneration of level splitting with formation of a high intensity absorption batochromic peak with doubled oscillator strength of transition. The red shift of this dimer state in vacuum takes place to 670 cm^{-1} if we include in the CI calculation the enlarged number of orbitals (for an example 15) to consider the more full account of electron exchange in the dimer excited state. From our point of view that situation corresponds to the formation absorption peak of J-aggregates, which has the additional red shift due to the surrounding of a high polarization medium in a thin solid film of dye.

The reason for the rotation at the dimerization of the PIC molecules is the influence of the two forces: the Coulomb interaction of the two cations and anions which try to bring the particles together and repulsive exchange interaction of the molecules' in the ground state . The overlap integral of the external π-electron orbitals of the carbon atoms and σ-electron

orbitals of the hydrogen atoms is decreasing at the rotation of the molecules to the perpendicular position of the molecules regarding each other. That leads to the decreasing of the repulsive part of the molecular interaction and the molecules are brought together until the new equilibrium between the forces is established.

3. Conclusion

The medium with the high polarizability compared with the polarizability of the dye in the solutions arises as a result of the dye thin solid film formation. This creates the condition for the appearance, as well the high negative value of the non-linear cubic susceptibility in resonance as the change of the sign on the dispersion curve of the cubic susceptibility and appearance the darkening on the long wavelength slope of the J-peak absorption. In the medium with high polarizability the considering of the four-level system for the J-aggregates excited state description is more appropriate compared with the two-level system typically considered for the J-aggregates. The depopulation of J-aggregate Frank-Condon excited state due to the appearance of lowered relaxed state leads to giant non-linear bleaching of J-aggregate peak and the excitation of the relaxed state leads to the non-linear absorption appearance. The value of non-linear response strongly depends on the relaxation time. The decrease of the relaxation time leads to the growth of non-linear response.

The increase of the medium polarizability enhances the non-linear response and is reflected in the increasing of the inhomogeneous broadening in the absorption and luminescence of the J-aggregates' spectra. The formation of the medium with high polarizability is clear seen from the spectral shift of the dye absorption during spin-coating and helps to explain the J-peak growth at the solid film formation. The inhomogeneous broadening in the J-peak absorption has the connection with aggregate thermal decay energy activation distribution and spectral inequivalent in the kinetics of the thermal decay of the J-aggregate absorption counter. The medium polarization influence on the optical and non-linear optical properties is important for the aggregated or supramolecular state of different dyes and nanostructures in the condensed phase.

The number of facts allow us to consider the properties of the pseudoisocyanine J-aggregates in the thin solid films as the properties of the strongly coupled dimers with inhomogeneous broadened spectral contour: the existence of the isobestic point at the J-aggregates' thermal conversion to monomer dye in the thin solid films or in the polymer films, the absence of the any hypsochromic spectral shift at the transition of the J-aggregate to monomer in the thin films at the addition of the octadecylquinolinium iodide, the high stabilization of the J-aggregate at the addition of the dipole closo-hydrodecaborate anion, the batochromic spectral shift of the J-peak at heating of the dye thin film, the narrowing of the J-peak in the thin solid films in the presence of organic cations and others.

The practical use of the obtained results on the non-linear properties is in the possible application of cyanine dyes' J-aggregates as the elements for teraherz demultiplexing of light signals and in schemes of ultra-short laser pulse stabilization (Plekhanov et al., 2004). The radiation stability of the J-aggregates is at a level of 0.5-1 MW/cm^2. This is useful to increase the radiation stability of the J-aggregates by 5-10 times. For safer J-aggregated films, application is enough to increase the thermal stability to 100-150^{o}C. However, the search for

new highly polarized aggregates of dyes with high absorption coefficients in the visible and infra-red spectral range that possess high thermal and photochemical stability remains a basic and practical task.

4. Acknowledgment

This study was supported by the Russian Foundation for Basic Research (project no. 02-03-33336), the programme "Fundamental Problems of Physics and Chemistry of Nanosystems and Nanomaterials" of the Presidium of the Russian Academy of Sciences (grant no. 8-2) and the programme of interdisciplinary integrated investigations of the Siberian Division of the Russian Academy of Sciences (project no. 84).

5. References

Arzhantsev, S., Ito, N., Heitz, M., Maroncelli, M. (2003). Solvation dynamics of coumarin 153 in several classes of ionic liquids: cation dependence of the ultrafast component. *Chem. Phys. Lett.* Vol. 381. pp. 278-286.

Bakalis, L. D. and Knoester, J. (2000). Linear absorption as a tool to measure the exciton delocalization length in molecular assemblies. *J. Lumin.* Vol. 87-89. pp.67–70.

Bakhshiev, N. G. Libov, V. S. Mazurenko, Yu. T. Amelichev, V. A. Saidov, G. V. and Gorodynskii, V. A. (1989). Solvation Chemistry: Problems and Methods [in Russian], Leningr. Gos. Univ., Leningrad (Rus.)

Blankenship, R.E., Olson, J.M., Miller, M. (1995). Antenna complexes from green photosynthetic bacteria, In: *Anoxygenic photosynthetic bacteria.* R.E. Blankenship, M.T. Madigan, and C.E. Bauer (eds.), Kluwer Academic Publish., Dordrecht, pp. 399-435.

Bogdanov, V.L., Viktorova, E N., Kulya, S V., and Spiro, A.S. (1991). Nonlinear cubic susceptibility and dephasing of exciton transitions in molecular aggregates, *JETP Letters*. Vol. 53, pp.105-108.

Burshtein, K. Ya., Bagaturyanz, A.A., Alfimov M.V. (1997). Computer modeling of the absorption line of the J-aggregates. *Izv. AN. ser. Khim* Vol.1. pp.67-69 (Rus.)

Cerasimova, T.N., Orlova, N. A., Shelkovnikov, V.V., Ivanova, Z. M., Markov, R. V., Plekhanov, A,I., Polyanskaya, T. M., Volkov, V. V. (2000). The Structure of Pseudoisocyanine Decahydro-*closo*-decaborate and Its Nonlinear Optical Properties in Thin Films. *Chemistry for Sustainable Development.* Vol.8, pp.109-114.

Coates, E. (1969). Aggregation of dyes in aqueous solution. *JSDS*. pp. 355-368.

Daltrozzo, E., Scheibe, G., Geschwind, K., Haimerl, F. (1974). On the structure of J-aggregates of pseudoisocyanine *Photogr. Sci. Eng*. Vol. 18. № 4. pp. 441-449.],

Das, K., Sarkar, N., Das, S., Datta, A., Bhattacharya, K. (1996). Solvation dynamics in solid host. Coumarin 480 in zeolite 13X. *Chem. Phys. Lett.* Vol. 249. pp. 323-328.

Ferrante, C., Rau, J., Deeg, F.W., Brauchle, C. (1998). Solvatation dynamics of ionic dyes in the isotropic phase of liquid crystals. *J. Luminesc.* Vol. 76-77. pp. 64-67.

Furuki, M., Tian, M., Sato, Y., Pu L.S. (2000). Terahertz demultiplexing by a single short time-to-space conversion using a film of squaryliun dye J-aggregates. *Appl. Phys. Lett*. Vol.77. pp.472-474.

Ghasemi, J.B., Mandoumi, N.A. (2008). New algorithm for the characterization of thermodynamics of monomer-dimer process of dye stuffs by photometric temperature titration. *Acta Chim. Slov.* Vol. 55. pp. 377-384.

Glaeske H., Malyshev V.A., Feller K.-H. (2001). Mirrorless optical bistability of an ultrathin glassy film built up of oriented J-aggregates: Effects of two-exciton states and exciton-exciton annihilation, *J. Chem. Phys.* Vol.114. pp.1966-1969

Guo, Ch., Aydin, M., Zyu, H-R., Akins, D.L. (2002). Density functional theory used in structure determinations and Raman band assignments for pseudoisocyanine and its aggregate. *J. Phys. Chem. B.* Vol.106. pp. 5447-5454

Herz, A.N. (1974). Dye-Dye interactions of cyanines in solution and at silver bromide surfaces. *Photogr. Sci. Engineering.* Vol. 18. №3. pp. 323-335

Jelley, E., (1936). Spectral absorption and fluorescence of dyes in the molecular state. *Nature,* Vol.138, pp. 1009-1010.,

Katrich, G.S., Kemnitz, K., Malyukin, Yu.V., Ratner, A.M. (2000). Distinctive features of exciton self-trapping in quasi-one-dimensional molecular chains (J-aggregates). *J. Luminesc*. Vol. 90. pp. 55-71

Kobayashi, T., ed. (1996). *J-aggregates*, World Scientific Publish. Co Pte. Ltd., Singapore.

Krasnov, K.S., (1984). *Molecules and chemistry bond*, High school. Moscow. (Rus.)

Kuhn, H., Kuhn, C. (1996). Chromophore coupling effects. In: *J-Aggregates.* T. Kobayashi (ed.)- Singapore: World scientific publishing Co. Pte. Ltd., - 228 p.

Lakowics, J.R. (1983). *Principles of fluorescence spectroscopy*. Plenum press. New York and London

Levshin, L.V., Salecky, A.M. (1989). *Luminescence measurement.* MGY. Moscow. (Rus.)

Mal'tsev E.I., Lypenko D.A., Shapiro B.I., and Brusentseva M.A. (1999). Electroluminescence of polymer/J-aggregate composites. *Appl. Phys. Lett.* Vol. 75, pp.1896-1898.

Malyshev, V.A. (1993). Localization length of one-dimensional exciton and low-temperature behaviour of radiative lifetime of J-aggregated dye solutions. *J. Luminesc.* Vol. 55. pp. 225-230.

Mandal, D., Sen, S., Bhattacharya, K., Tahara, T. (2002). Femtosecond study of solvation dynamics of DCM in micelles. *Chem. Phys. Lett.* Vol. 359. pp. 77-82.

Markov, R. V., Chubakov, P. A., Plekhanov, A. I., Ivanova, Z. M., Orlova, N. A., Gerasimova, T. N., Shelkovnikov, V. V., and Knoester, J. (2000). Optical and nonlinear optical properties of low-dimensional aggregates of amphyphilic cyanine dyes. *Nonlinear Opt.*, Vol.25, pp.365–371

Markov, R.V., Plekhanov, A.I., Rautian, S.G., Orlova, N.A., Shelkovnikov, V.V., Volkov, V.V. (1998). Nonlinear optical properties of two types of PIC J-aggregates in thin films. *Proc. SPIE.* Vol. 3347. pp. 176-183. (a)

Markov, R.V., Plekhanov, A.I., Rautian, S.G., Orlova, N.A., Shelkovnikov, V.V., Volkov, V.V. (1998). Nonlinear optical properties of the two types pseudoisocyanine J-aggregates in thin films. *Jurnal Nauchn. and Prikl. Fotogr.* Vol. 43. pp.41-47. (Rus.) (b)

Markov, R.V., Plekhanov, A.I., Rautian, S.G., Safonov, V.P., Orlova, N.A., Shelkovnikov, V.V., Volkov, V.V. (1998). Dispersion of cubic susceptibility of thin films of pseudoisocyanine J-aggregates as measured by longitudinal scanning, *Optics and Spectroscopy*. Vol. 85. pp.588-594. (c)

McDermott, G., Prince, S.M., Freer, A.A. et al., (1995). Crystal structure of an integral membrane light-harvesting complex from photosynthetic bacteria, *Nature*. Vol.374. pp. 517-521.

Minoshima, K., Taiji, M., Misawa K. and Kobayashi, T. (1994). Femtosecond nonlinear optical dynamics on excitons in J-aggregates. *Chem. Phys. Lett.* Vol.218. pp.67–72

Moll, J., Daehne, S., Durrant, J. R. and Wiersma, D. A. (1995). Optical dynamics of excitons in J-aggregates of carbocyanine dye. *J. Chem. Phys.* Vol.102. No. 16. pp.6362–6370

Nygren, J., Andrade, J. M., Kubista, M. (1996). Characterization of a single sample by combining thermodynamic and spectroscopic information in spectral analysis. *Anal. Chem.* Vol. 68. pp. 1706-1710.

Orlova, N.A., Kolchina, E.F., Zhuravlev, F.A., Shakirov, M.M., Gerasimova, T.N., Shelkovnikov, V.V.(2002). Synthesis of 2,2′-quinocyanines with long alkyl groups. *Chemistry Heterocyclic Compounds*. № 10, pp. 1399-1407. (Rus.)

Orlova, N.A., Zhuravlev, F.A., Shelkovnikov, V.V., Gerasimova, T.N. (1995). Synthesis of pseudoisocyanines with nonsaturated groups in position 1. *Izv. AN, ser, khim.* № 6, pp. 1122-1124 (Rus.)

Pilling, R.L., Hawthorne, M.F. (1964). The boron-11 nuclear magnetic resonance spectrum of $B_{20}H_{18}^{-2}$ at 60 Mc./sec.*J. Amer. Chem. Soc.* p Vol. 86. pp. 3568-3569.,

Plekhanov A.I., Rautian S.G., Safonov V.P., (1995). *Optics and Spectroscopy* Vol.78, 1, p.92. .(Rus.)

Plekhanov, A.I., Kuch'yanov, A.S., Markov, R.V., Simanchuk, A.E., Avdeeva, V.I., Shapiro, B.I., Shelkovnikov, V.V. (2004). Passive mode locking of a Nd3+:YAG laser with a saturable absorber in the form of thin film of J-aggregates. J. *Nonlinear Org. and Polymer Materials.* Vol. 9. № 3. pp. 503–511.

Plekhanov, A.I., Orlova, N.A., Shelkovnikov, V.V., Markov, R.V., Rautian, S.G., Volkov, V.V. (1998). Third-order non-linearity optical properties of the film of the cyanine dye with borate anion. *Proc. SPIE*. Vol. 3473. pp. 100-107. (a)

Plekhanov, A.I., Rautian, S.G., Safonov, V.P., Chubakov, P.A., Orlova, N.A., Shelkovnikov, V.V (1998). Dispersion of the real and imaginary parts of cubic susceptibility in submicron films of pseudoisocyanine J-aggregates. *Proc. SPIE*. Vol. 3485. pp. 418-424.(b)

Plekhanov, A.I., Markov, R.V., Rautian, S.G., Orlova, N.A., Shelkovnikov, V.V., Volkov, V.V (1998). Third-order nonlinearity optical properties of the films of cyanine dye with borate anion. *Proc. SPIE "Third-Order Nonlinear Optical Materials"*. Vol. 3473. pp. 20-31.(c)

Renge, I., Wild, U.P. (1997). Solvent, temperature, and excitonic effects in the optical spectra of pseudoisocyanine monomer and J-aggregates. *J. Phys. Chem. A*. Vol. 01. pp. 7977-7988.

Saha, S., Mandal, P.K., Samanta, A. (2004). Solvation dynamics of Nile Red in a room temperature ionic liquid usingstreak camera. *Chem. Phys.* Vol. 6. pp. 3106-3110.

Sato, T., Yonezawa, Y., Hada, H. (1989). Preparation and luminescence properties of J-aggregates of cyanine dyes at the phospholipid vesicle surface. *J. Phys. Chem.* Vol. 93. pp. 14-16.

Scheibe, G., (1936). Variability of the absorption spectra of some sensitizing dyes and its cause. *Angew. Chem,* Vol.49, p. 563.

Shapiro, B.I. (1994) Aggregates of cyanine dyes: photographic problems, *Russian Chemical Reviews.* Vol.63. pp.231-241.

Shelkovnikov, V. V., Ivanova, Z. M., Orlova, N. A., Volkov, V. V., Drozdova, M. K., Myakishev, K. G., Plekhanov, A. I.(2004). Optical Properties of Solid Pseudoisocyanine Films Doped with Cluster Derivatives of Boron Hydrides. *Optics and Spectroscopy*. Vol. 96, pp.824-833

Shelkovnikov, V.V., Plekhanov, A.I., Safonov, V.P., Zhuravlev, F.A. (1993) Nonlinear optical properties of the assembliesof organic molecules and fractal metal clusters. *Zhurnal struct. chem*. Vol.34. pp.90-105 (Rus.)

Shelkovnikov,V. V., Ivanova, Z. M., Orlova, N. A., Gerasimova, T. N., Plekhanov, A. I. (2002). Formation and properties of long alkyl substituted pseudoisocyanines J-aggregates in thin films. *Optics and Spectroscopy*. Vol.92. pp. 958–966

Struganova, I. (2000) Dynamics of formation of 1,1'-diethyl-2,2'-cyanide iodide J-aggregates in solution. *J. Phys. Chem. A.* Vol. 104. № 43. pp. 9670-9674.

Sundstrom, V., Gillbro, T., Gadonas, R.A., Piskarskas, A. (1988). Annihilation of singlet excitons in J-aggregates of pseudoisocyanine (PIC) studied by pico- and subpicosecond spectroscopy. *J. Chem. Phys.* Vol. 89. № 5. pp. 2754-2762.

Suppan, P. (1990). Solvatochromic shifts - the influence of the medium on the energy of electronic states. *J. Photochem. Photobiol. A: Chemistry.* Vol. 50. pp.293-330.

Tani, I.., Liu-Yi, Sasaki, F., Kobayashi, S., Nakatsuka, H. (1996). Persistent spectral hole-burning of pseudoisocyanine bromide J-aggregates. *J. Luminesc.* № 66-67. pp.157-163.

Tani, T. (1996) J-aggregates in spectral sensitization of photographic materials, In: *J-aggregates*. T. Kobayashi (ed.). World Scientific Publish. Co Pte. Ltd., Singapore. pp. 209-228.,

Tikhonov, E.A., Shpak, M.T. (1977). *Nonlinear optical phenomena in organic compounds*. Naukova dumka. Kiev.

Tretiak, S., Saxena, A., Martin, R. L., and Bishop, A. R. (2000). Interchain Electronic Excitations in Poly(phenylenevinylene) (PPV) Aggregates. *J. Phys. Chem. B*, Vol.104, pp.7029-7037

Trosken, B., Willig, F., Spitle, R. M. (1995) The primary steps in photography: excited J-aggregates on AgBr microcrystals, *Advanced Material*s, Vol. 7, pp. 448-450. ,

Vacha, M., Furuki, M., Tani, T. (1998). Origin of the long wavelength fluorescence band in some preparations of J-aggregates low-temperature fluorescence and hole burning study. *J. Phys. Chem. B.* Vol. 102. pp. 1916-1919.,

Verezchagin A.N. (1980). *Polarisability of molecules*. Nauka. Moskow. (Rus.)

Wang Y. (1991) Resonant third-order optical nonlinearity of molecular aggregates with low-dimensional excitons, *Journal of the Optical Society of America B*. Vol.8, pp.981-990.,

Warshell A. (1977). The self-consistent force field method and quantum chemical generalization, In: *Semiempirical methods of electronic structure calculation*. Segal. G.A. (ed.). Plenum press. New York and London

Wendlandt W.W. (1974). *Thermal Methods of Analysis*. John Wiley & Sons, Inc. New York.

Wurthner, F., Kaiser, Th.E., Saha-Moller, Ch.R. (2011). J-Aggregates: From Serendipitous Discovery to Supramolecular Engineering of Functional Dye Materials. *Angew. Chem. Int. Ed.* Vol.50. pp. 3376 – 3410.

Zhuravlev, F.A., Orlova, N.A., Shelkovnikov, V.V., Plekhanov, A.I., Rautian, S.G., Safonov, V.P. (1992)Giant non-linear susceptibility of the thin films with complexes molecular aggregate – metal cluster. *Pis'ma JETF* . Vol.56. pp.264-267 (Rus.)

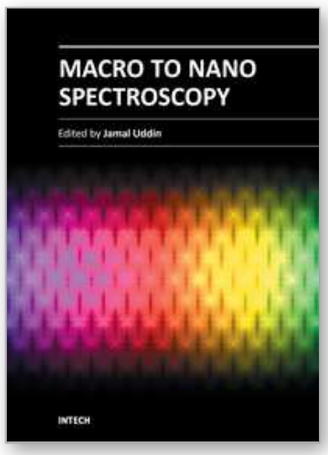

Macro To Nano Spectroscopy

Edited by Dr. Jamal Uddin

ISBN 978-953-51-0664-7
Hard cover, 448 pages
Publisher InTech
Published online 29, June, 2012
Published in print edition June, 2012

In the last few decades, Spectroscopy and its application dramatically diverted science in the direction of brand new era. This book reports on recent progress in spectroscopic technologies, theory and applications of advanced spectroscopy. In this book, we (INTECH publisher, editor and authors) have invested a lot of effort to include 20 most advanced spectroscopy chapters. We would like to invite all spectroscopy scientists to read and share the knowledge and contents of this book. The textbook is written by international scientists with expertise in Chemistry, Biochemistry, Physics, Biology and Nanotechnology many of which are active in research. We hope that the textbook will enhance the knowledge of scientists in the complexities of some spectroscopic approaches; it will stimulate both professionals and students to dedicate part of their future research in understanding relevant mechanisms and applications of chemistry, physics and material sciences.

InTech Europe
University Campus STeP Ri
Slavka Krautzeka 83/A
51000 Rijeka, Croatia
Phone: +385 (51) 770 447
Fax: +385 (51) 686 166
www.intechopen.com

InTech China
Unit 405, Office Block, Hotel Equatorial Shanghai
No.65, Yan An Road (West), Shanghai, 200040, China
中国上海市延安西路65号上海国际贵都大饭店办公楼405单元
Phone: +86-21-62489820
Fax: +86-21-62489821

IntechOpen